

# SAE Aero Design Knowledge, 2021



**School Name:** Dwarkadas J. Sanghvi College of Engineering

**Team Name:** DJS SKYLARK - REGULAR CLASS

**Team Number:** 019

## Team Members

**Team Captain:** Shome Vakharia

Aaryan Shah	Jinay Gandhi	Roshan Sam
Abhimanyu Suthar	Joel Ponmany	Sharva Potdar
Abhishek Malichkar	Kenith Shah	Shikha Punjabi
Arshish Balaporia	Kirtan Jhaveri	Shlok Mandloi
Aryan Ashar	Lobhas Patankar	Shubham Mody
Aryan Thukral	Nainika Shah	Tanmay Kshire
Harshal Soni	Neel Mehta	Ved Vartak
Hiral Shah	Neil Vashani	Vighnesh Patil
	Parv Khandelwal	
	Radhika Puranik	
	Raj Anadkat	
	Rishi Ghia	

## STATEMENT OF COMPLIANCE

### Certification of Qualification

Team Name DJS Skylark – REGULAR CLASS Team Number 019  
School Dwarkadas J. Sanghvi College of Engineering  
Faculty Advisor Prof. Shashikant Auti  
Faculty Advisor's Email shashikant.auti@gmail.com

### Statement of Compliance

As faculty Adviser:

SMA (Initial) I certify that the registered team members are enrolled in collegiate courses.

SMA (Initial) I certify that this team has designed and constructed the radio-controlled aircraft in the past nine (9) months with the intention to use this aircraft in the 2021 SAE Aero Design competition, without direct assistance from professional engineers, R/C model experts, and/or related professionals.

SMA (Initial) I certify that this year's Design Report has original content written by members of this year's team.

SMA (Initial) I certify that all reused content have been properly referenced and is in compliance with the University's plagiarism and reuse policies.

SMA (Initial) I certify that the team has used the Aero Design inspection checklist to inspect their aircraft before arrival at Technical Inspection and that the team will present this completed checklist, signed by the Faculty Advisor or Team Captain, to the inspectors before Technical Inspection begins.



Signature of Faculty Advisor

25/02/2021

Date



Signature of Team Captain

28/02/2021

Date



## Table of Contents

<b>List of Figures, Tables, Symbols, and Abbreviations</b>	<b>2</b>
<b>1.0 Executive Summary</b>	<b>3</b>
1.1 System Overview and Discriminators	3
1.2 Competition Projections	4
<b>2.0 Project Management</b>	<b>4</b>
2.1 Schedule Summary	4
2.2 Personnel Management	5
2.3 Cost Report	5
2.4 Risk Analysis	6
<b>3.0 Design Layout and Trades</b>	<b>6</b>
3.1 Overall Design Features and Details	6
3.2 Competitive Scoring Strategy and Analysis	9
3.3 Design Derivations	12
3.4 Interfaces and Attachments	15
<b>4.0 Loads, Environments and Assumptions</b>	<b>16</b>
4.1 Design Load Derivations	16
4.2 Environmental Considerations	17
<b>5.0 Analyses</b>	<b>17</b>
5.1 Analytical Tools	17
5.2 Developed Models	18
5.3 Performance Analyses	19
5.3.1 Dynamic Thrust	19
5.3.2 Take-off and Climb-out Performance	19
5.3.3 Flight and Maneuver Performance	20
5.3.4 Static and Dynamic Stability	20
5.3.5 Payload Prediction Analysis	21
5.3.6 Drag Polar Analysis	21
5.4 Structural Analyses	21
5.4.1 Critical Margins	21
5.4.2 Applied Loads and Material Selection	22
<b>6.0 Sub-assembly Tests and Integration</b>	<b>24</b>
<b>7.0 Manufacturing</b>	<b>25</b>
<b>8.0 Conclusion</b>	<b>25</b>
Appendix A – Backup Calculations	26
Appendix B – Technical Data Sheet	
2D Drawing	



## List of Symbols

C	Chord of the control surface	S <sub>1</sub>	Maximum control surface deflection
C <sub>D</sub>	Drag coefficient of aircraft	S <sub>2</sub>	Maximum servomotor deflection
C <sub>Di</sub>	Lift-induced drag coefficient	S <sub>T0</sub>	Take-off Distance
C <sub>D0</sub>	Zero-lift drag coefficient	T <sub>s</sub>	Static Thrust
C <sub>f</sub>	Skin friction drag coefficient	T <sub>d</sub>	Dynamic Thrust
C <sub>L</sub>	Lift coefficient of aircraft	v	Airspeed
C <sub>M</sub>	Coefficient of pitching moment of aircraft	v <sub>d</sub>	Dive speed
D	Drag	v <sub>e</sub>	Exit Velocity
g	Acceleration due to Gravity	v <sub>gE</sub>	Gust Velocity
k <sub>g</sub>	Gust coefficient	W	Weight of the aircraft
L	Lift	α	Angle of attack
m	Mass of the aircraft	ρ	Density
n	Load factor	ω	Frequency
S	Wing Planform Area	Φ	Aircraft Bank Angle

## List of Abbreviations

AR	Aspect Ratio	DA	Density Altitude
CAD	Computer Aided Drawing	FoS	Factor of Safety
CFD	Computational Fluid Dynamics	MoS	Margin of Safety
CG	Centre of Gravity	TMA	Tail Moment Arm

## List of Figures and Tables

Figure 1(a)	System Overview and Discriminators	Figure 4(c)	Environmental Considerations
Table 1(b)	Subsystem Details	Chart 5(a)	Developed Model
Figure 2(a)	Schedule Summary	Figure 5(b)	Dynamic Thrust Performance
Figure 2(b)	Schedule and Cost Breakdown	Figure 5(c)	Take-off and Climb Out Telemetry
Table 2(c)	Risk Analysis	Table 5(d)	Post Flight-Test Optimization
Figure 3(a)	Wing Layout	Figure 5(e)	Minimum Turning Radius
Figure 3(b)	Fuselage Layout	Figure 5(f)	Maximum Banking Angle
Figure 3(c)	Empennage Layout	Table 5(g)	Stability Response
Figure 3(d)	Avionics System Layout	Figure 5(h)	Short Period and Phugoid Modes
Figure 3(e)	Sensitivity Analysis	Table 5(i)	Lateral Stability Eigenvalues
Figure 3(f)	Planform Analysis	Figure 5(j)	Drag Polar Analysis
Figure 3(g)	Cargo Configuration Analysis	Table 5(k)	Material Selections
Figure 3(h)	Overall Scoring Strategy	Figure 5(l)	Crosswind Analysis
Figure 3(i)	High Lift Devices	Figure 5(m)	Composite Stress Analysis
Figure 3(j)	C <sub>M</sub> vs α	Figure 5(n)	Weight Distribution
Figure 3(k)	Motor-Propeller Combinations	Table 6(a)	Servo Torque Requirements
Figure 4(a)	V-n Diagram	Chart 7(a)	Manufacturing Process
Table 4(b)	Landing Shock Calculations		



## 1.0 Executive Summary

### 1.1 System Overview and Discriminators

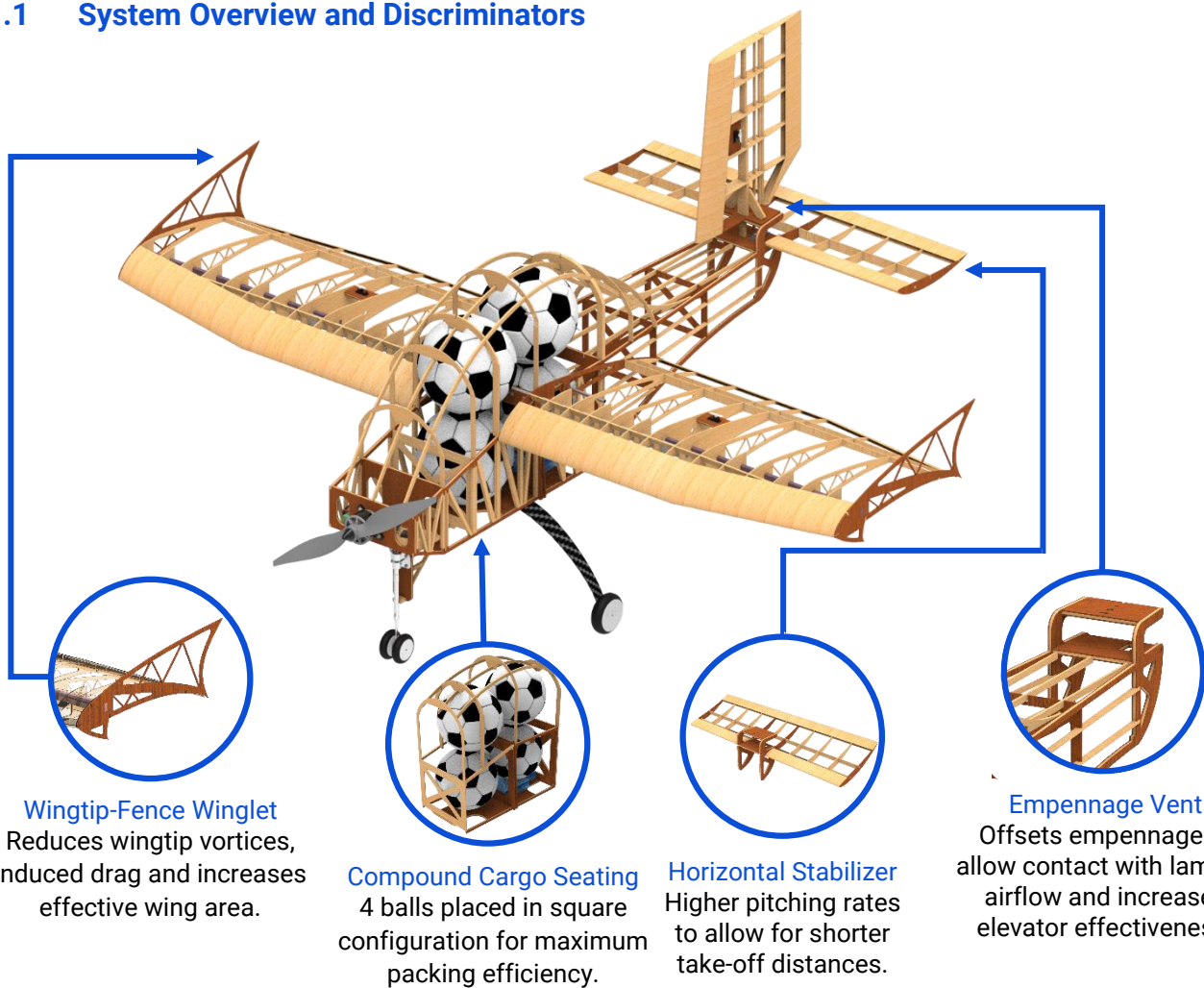


Figure 1(a): System Overview and Discriminators

Avionics		
Motor	Propeller	Battery
Sunny Sky X5320 250kV	APC 21x12 WE	Tattu LiPo 3300mAh 6S
Wings		
Airfoil	Span	Planform
S1223 RTL	80in	Recto-Trapezoidal
Empennage		
Horizontal Tail Airfoil	Vertical Tail Airfoil	Configuration
AH 79-100C	NACA0009	Inverted T Tail
Scoring Strategy		
Spherical Cargo Lifted	Configuration	Boxed Cargo Lifted (lbs.)
4 Soccer Balls	Square (   to Longitudinal Axis)	10.5

Table 1(b): Subsystem Details

## 1.2 Competition Projections

The team designed the aircraft to carry 14 lbs. of total cargo weight, comprising 4 Soccer Balls and 10.5 lbs. of Boxed Cargo: achieving a projected score of 27.601 points per round and 92.805 points in total including the Payload Prediction bonus. Combining our flight scores with strong Design Report and Technical Presentation scores, we aim to place in the Top 3 Overall. We obtained these scores by performing in-depth sensitivity analysis on the scoring equation to understand which parameters to optimize, followed by extensive trade studies for each component based on the results obtained from the former, along with repeated empirical tests.

## 2.0 Project Management

### 2.1 Schedule Summary

The COVID-19 pandemic and the resulting lockdown in India heavily affected the team's schedules and ability to manufacture and test prototypes throughout the year. Work began in November as the restrictions were relaxed until which, we invested all our time in training new recruits and researching different designs and ideas. We based our schedules on cycles of design, testing and optimization working around our exam schedule. 4 prototypes were built and tested with each bringing into the foray a slew of improvements and optimizations.

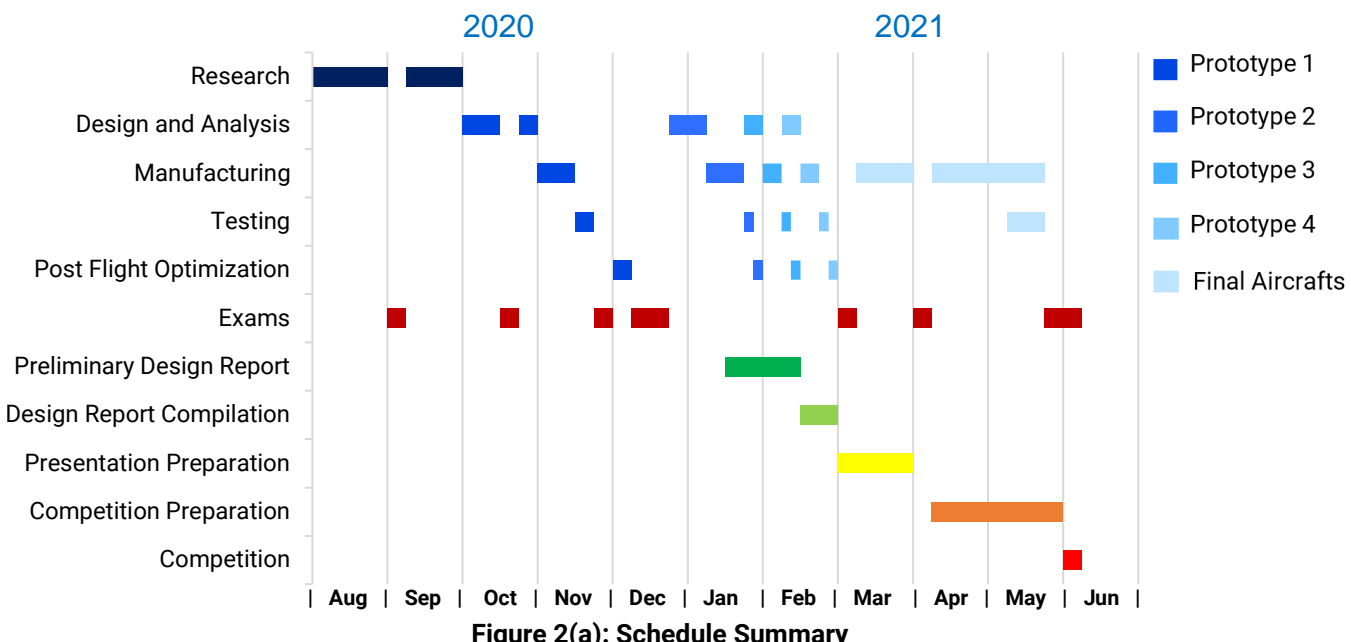
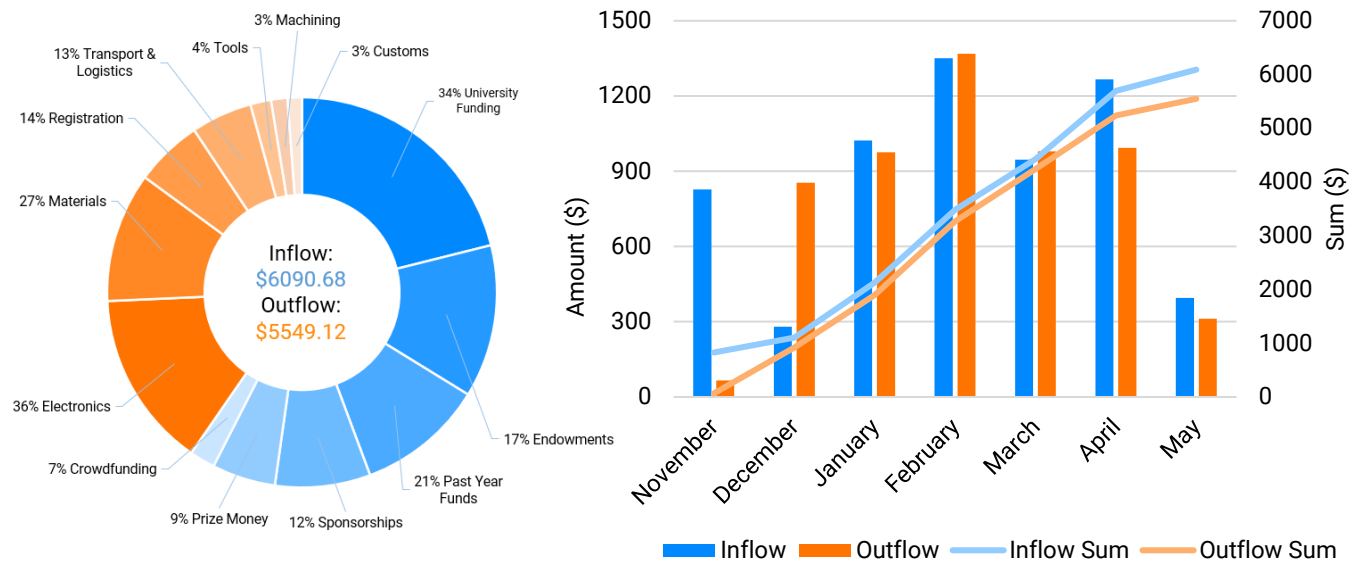


Figure 2(a): Schedule Summary

## 2.2 Personnel Management

Comprising of 29 students, the team was segregated into aerodynamics, structures, avionics, and marketing departments; ensuring ideas could be shared and discussed effectively inter and intra-departmentally, allowing for progress in designs for both Regular and Micro classes. Over time, Design Report and Technical Presentation groups were formed.

## 2.3 Cost Report



**Figure 2(b): Schedule and Cost Breakdown**

COVID-19 heavily affected the team's inflow of funds starting with delayed and reduced university funding and crowdfunding, close to no sponsorships as well as cancellation of the annual aero-modelling workshop the team conducts to raise a significant percentage of its funds annually. The outflow of funds largely comprised of electronic components, raw material procurement, manufacturing tools, registration fee and logistics. To reduce the high costs of material procurement, we contacted international wholesalers directly. High customs duty, long shipping periods and product unavailability worldwide limited our options for testing electronics, which we overcame by using online tools to shortlist components before testing. Figure 2(b) represents how funds were managed through the year to eliminate any financial blockages in the design process and manufacturing.

## 2.4 Risk Analysis

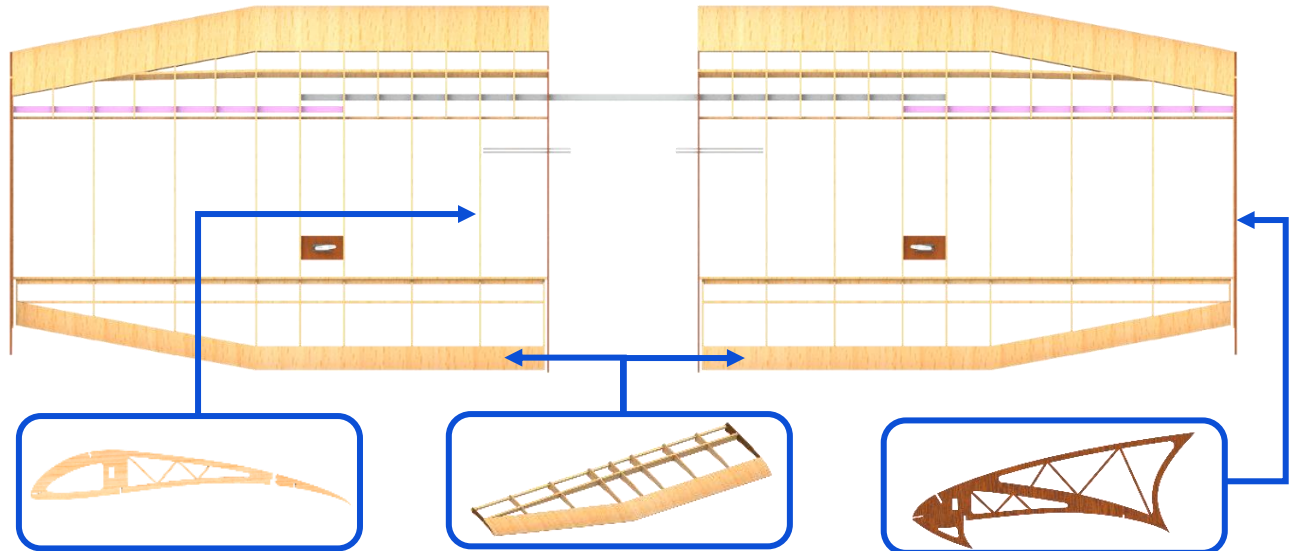
Risk Factor	Probability of Occurrence	Impact	Mitigation
Crosswinds and Gusts	High	High	Minimize longitudinal section area and improve rudder performance
Wing and Tail Strikes	Low	Medium	Addition of a wingtip fence to prevent wing strikes and curvature of fuselage to prevent tail strikes
High Impact Landing Shocks	Medium	High	Used a carbon fiber main landing gear and a nose landing gear with a telescopic suspension
Servo and Control Surface Failure	Low	Medium	Combined use of other control surfaces to make the airplane glide to safety
Structural Component Failure	Low	High	Choose materials with a high tensile strength and assemble fuselage with a strong bonding agent and cyanoacrylates
Material Acquisition Delays	High	High	Use materials and components sparingly and contacting personal acquaintances while ordering
Monetary Constraints	High	High	Acquire funds through individual member contributions and a crowdfunding campaign

Table 2(c): Risk Analysis

## 3.0 Design Layout and Trades

### 3.1 Overall Design Features and Details

#### 3.1.1 Wings



**Airfoil Shaped Ribs**  
S1223-RTL with 24" root chord and 18" tip chord used. Weight reductions implemented; trusses added with differing grain direction for high load bearing capability.

**Flaperon**  
Reduces take-off distance; covers 20% of wing area.  
Extends for the entire span for high rolling moments & high lift due to propwash.

**Wingtip-Fence Winglet**  
Protects from wingtip strikes, allows for smaller upper section by moving leakage of high-pressure air behind

Figure 3(a): Wing Layout

The team opted for a recto-trapezoidal planform where the rectangular section provides comparatively high lift within the region affected by propwash, while the tapered section has substantially lesser induced drag and assists in achieving the velocities required for takeoff. The

wing is made of airfoil-shaped ribs, retained in place with balsa jigs and a main spar with hollow aluminum in the center and XPS foam to the sides to sustain in-flight loads while maintaining a low empty weight.

### 3.1.2 Fuselage and Landing Gear

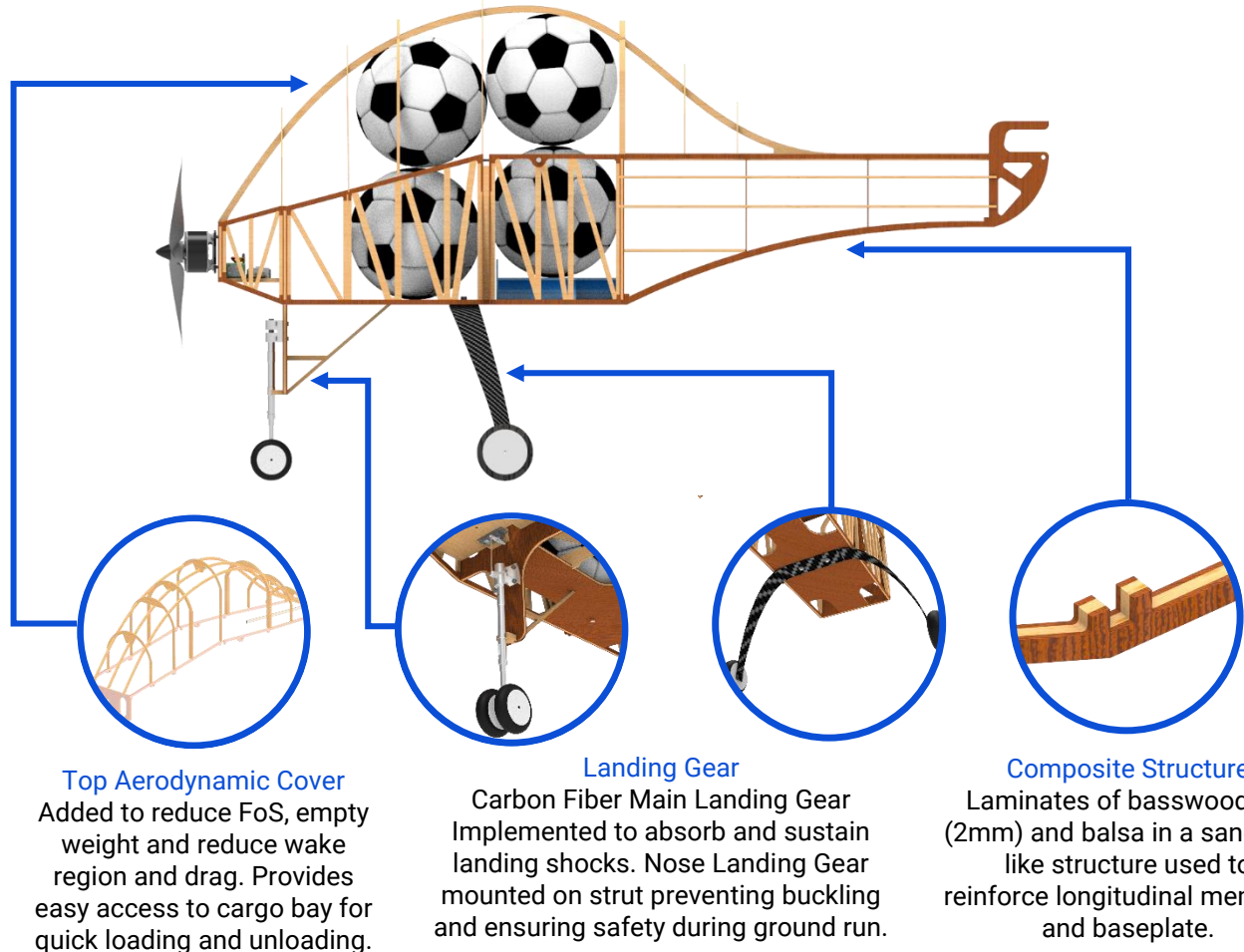


Figure 3(b): Fuselage Layout

We designed the fuselage as a chassis structure with detachable auxiliary aerodynamic covers comprising three sections for ease of manufacturing -- the nose, mid, and tail sections. The tail section is tapered to prevent tail-strikes and reduce area to avoid unnecessary yaw. A top aerodynamic cover allows for lesser drag and a smaller wake region while reducing the load bearing components in the fuselage, thereby decreasing FoS from 3.715 to 1.508 and saving on empty weight. A tricycle landing gear is used owing to its immunity to ground looping. The Main

Landing Gear has a Carbon Fiber structure to resist landing impacts and reduce empty weight while the Nose Landing Gear is made of aluminum with a spring-loaded suspension.

### 3.1.3 Boxed and Spherical Cargo

As per **Section 1.2**, we decided to go for a 4-ball strategy with 10.5 lbs. of boxed payload in the form of mild steel plates of dimensions 5.59in x 5in x 0.157in and 2.91in x 2.5in x 0.157in. The spherical balls majorly influence CG and are therefore placed in close proximity to the desired CG, retained laterally by longerons and longitudinally by ribs in the fuselage structure. Efficient packaging, ease of loading and machinability of steel plates were given priority, their dimensions being derived primarily from the dimensions of the spherical balls to minimize longitudinal sectional area of the fuselage. The top aerodynamic cover hinged at the motor mount rib opens to facilitate loading and unloading of cargo efficiently.

### 3.1.4 Empennage

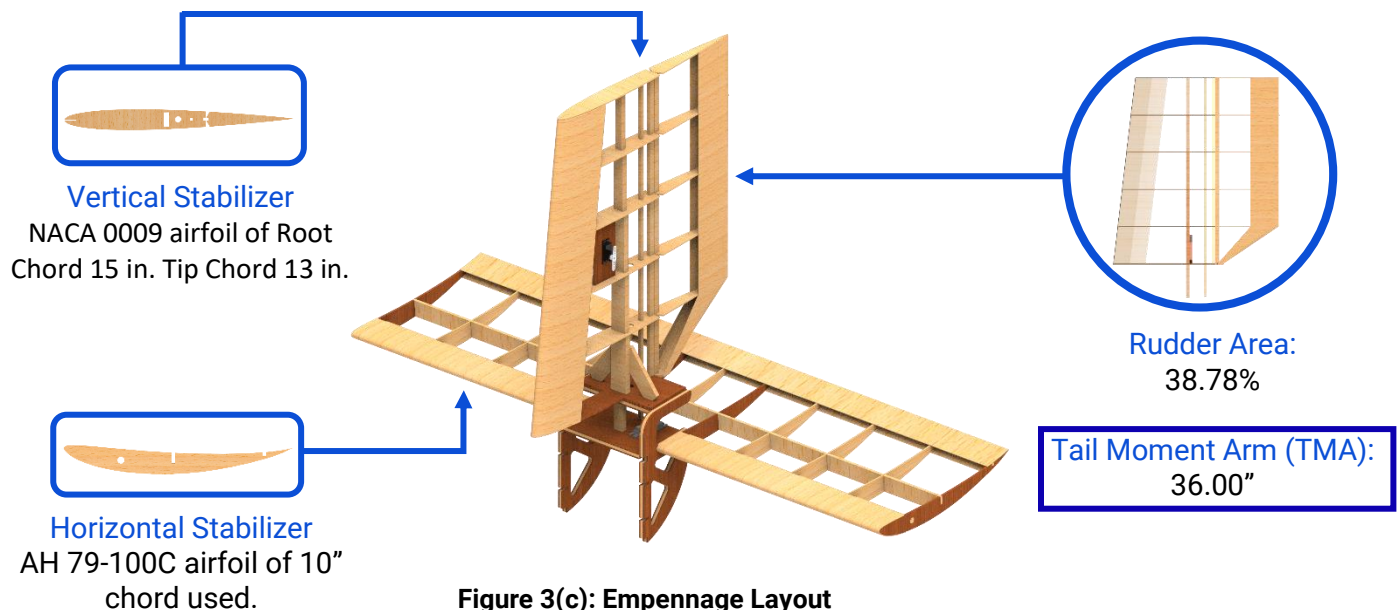
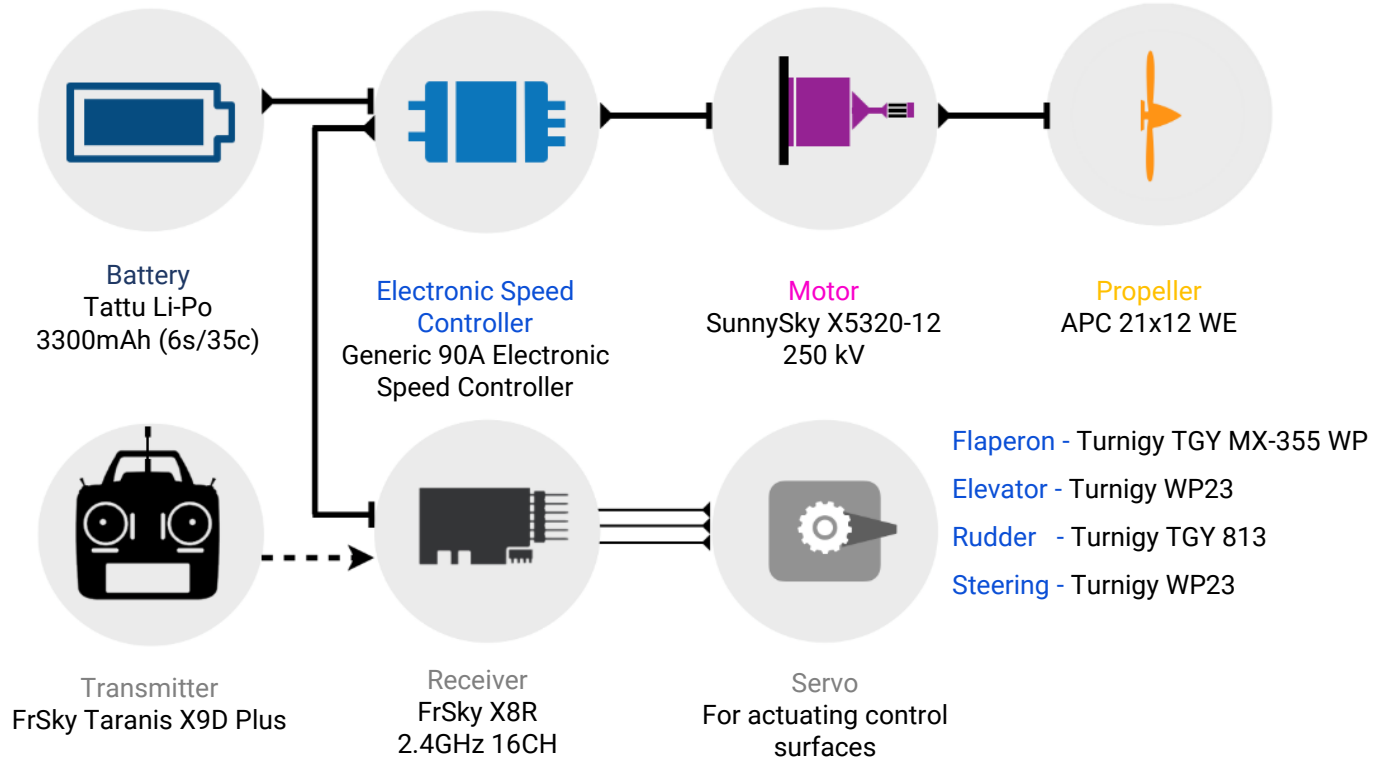


Figure 3(c): Empennage Layout

The aircraft utilizes an inverted T-Tail configuration for its reliability while reducing empty weight by 40% as compared to a U-Tail. We decided to use the horizontal stabilizer as a control surface, giving us higher pitching moments compared to a conventional elevator arrangement. A

staggered primary spar was used, getting progressively thicker from the top to bottom to provide structural reinforcement at the base.

### 3.1.5 Avionics



**Figure 3(d): Avionics System Layout**

### 3.2 Competitive Scoring Strategy and Analysis

The optimization goal of the scoring equation is to maximize the numerator, i.e., Number of balls and payload, and to minimize the denominator i.e., Span and cargo bay length. In order to accomplish this while keeping in mind the 100ft. takeoff distance and 1000W power limit, we performed an exhaustive search in the domain to find the optimal wing planform and cargo configurations. As the planform and cargo configurations are independent of each other, it is possible to optimize them individually, and combine their effects to obtain the overall scoring strategy.

### 3.2.1 Planform Analysis

We curated a database of multiple airfoils to maximize lift, airfoil efficiency, and stall angle, while minimizing drag. Of these, S1223RTL was found to perform the best overall. Subsequently, we ran the Tornado VLM Solver in MATLAB on over 1100 wing planforms with varying dimensions of Root Chords 14-24in, Tip Chords 10-20in, Spans 60-120in, Rectangular percentages 20-80%, Angles of Incidence 0-10° and Aspect Ratios 3-7. Later, the top 10% configurations of each span were shortlisted, and high meshing Solidworks CFD Analyses were run on them for more accurate results. We factored in the empty weight increase for wingspans by calculating the quantity of balsawood used; evaluating the mass properties provided by our CADs. The Lift and Drag values obtained were used as inputs to our score and take off distance calculator (**Section 5.2**).

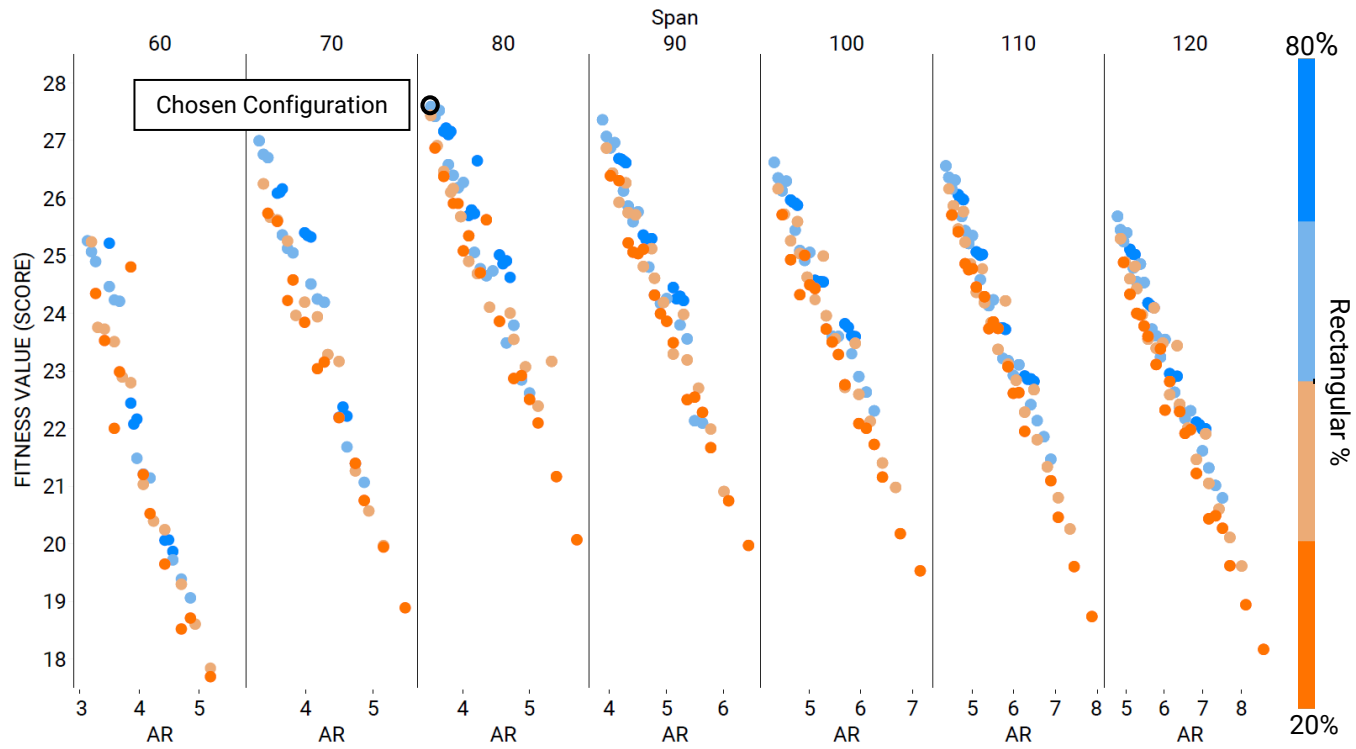


**Figure 3(e): Planform Analysis**

As cargo configuration and empty weight were kept constant, we could compare performance effectively. Scores have been plotted above with each of the 1100 data points representing one planform. Lower aspect ratios and higher rectangular percentages with spans ranging from 70-

90 in. have the best scoring characteristics owing to higher lift despite increased drag. Hence, we chose to maximize allup weight lifted, compromising on the drag, to reduce the span penalty on the scoring equation. The final planform selected has a span of 80in, Root and Tip Chord 24 and 18in, Rectangular percentage of 60% and an AR of 3.508 yielding a score of 27.601 points with the selected cargo configuration of 4 balls + 10.5 lbs. of boxed cargo.

### 3.2.2 Cargo Config Analysis

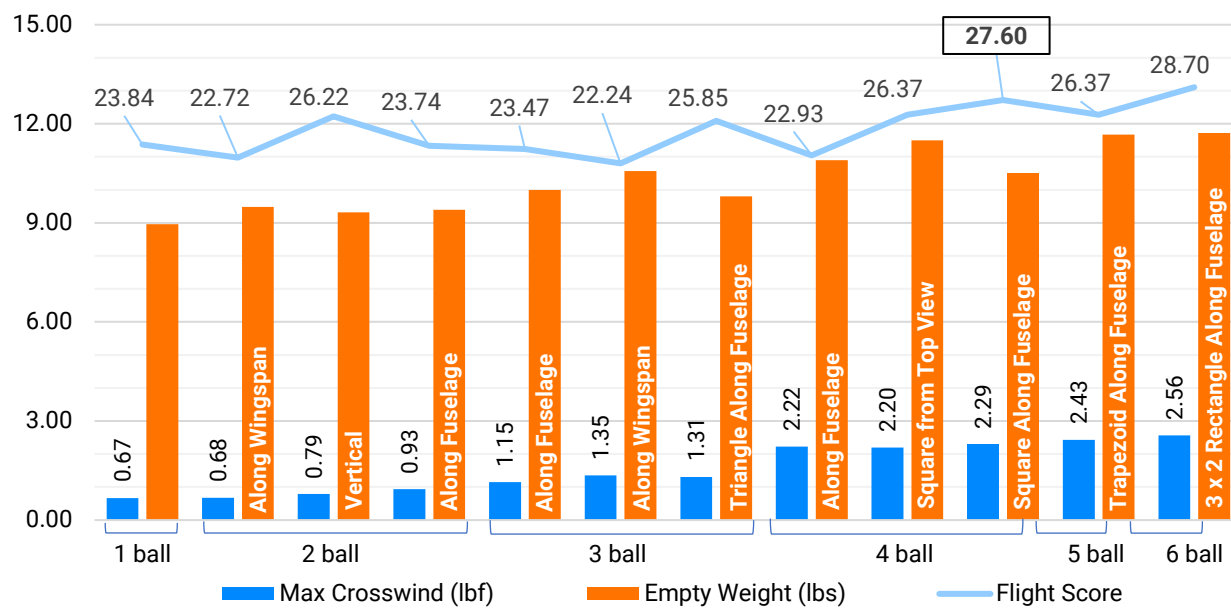


Figure 3(f): Cargo Configuration Analysis

To select the cargo configuration, the team calculated scores for each fuselage and ball configuration keeping the wing planform constant, plotting them against their respective crosswind performance and empty weights (derived from CADs and scaled down test sections). The change in multiplier from 2 to 3 made multiple ball configurations much more viable. 3 and 5-ball configurations are filtered out for their inefficient use of cargo bay length and negligible crosswind performance improvements. Thus the 4-ball square configuration along the fuselage was chosen for its efficient use of cargo bay length and competitive score, while still being safely maneuverable in adverse crosswind conditions as discovered after extensive flight testing.

### 3.2.3 Overall Scoring Strategy

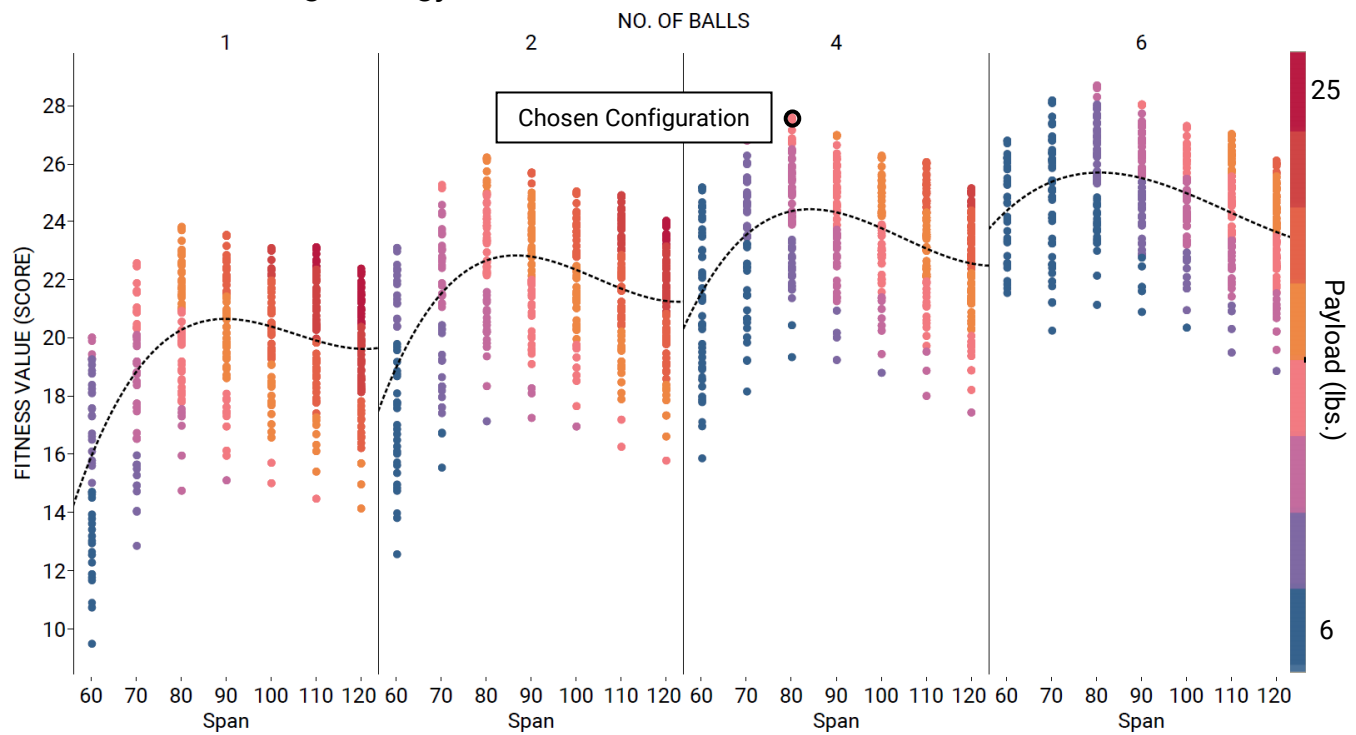


Figure 3(g): Overall Scoring Strategy

The graph compares the scores of each planform with shortlisted cargo configurations from **Section 3.2.2** against span. The team divided the scoring strategy into two sections, **Planform Analysis** and **Cargo Configuration Analysis**. While varying one, the other was kept constant, allowing for effective and direct comparisons. The wing planform lifting the highest all-up weight within 100ft was chosen, regardless of cargo configuration; and the cargo configuration was chosen such that it utilized the all-up weight the most effectively, giving us the optimal score.

## 3.3 Design Derivations

### 3.3.1 Wings

The team built 4 prototypes, testing high-lift devices, materials, planforms, and mountings. The first wing was devoid of any high-lift devices to obtain a performance baseline. As the design progressed, we tested winglets, vortex generators and flaperons, which increased score, delayed stall, and reduced drag. The high FoS of the first wing was reduced with each iteration; replacing the outer half of the aluminum spar with XPS foam, adding half-airfoil ribs to retain shape while

reducing weight, and adding trusses to ribs to reduce weight and increase strength. We chose the mid-wing mount over low and high wing mounts, as it increased the wing area in propwash and provided us with a feasible compromise between ground effect and stability.

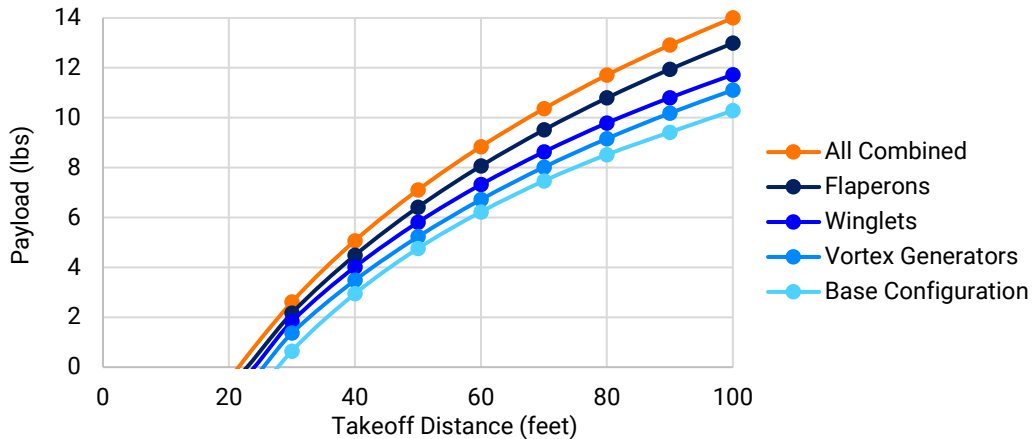


Figure 3(h): High Lift Devices

### 3.3.2 Fuselage

The primary dimensions of the fuselage were derived by satisfying the required TMA, CG position, electronics, and payload bay capacities. The longerons, ribs and baseplate were made of a basswood-balsa-basswood composite of 3–3–3 mm which was made 2–4–2 mm to reduce FoS and empty weight. The fuselage longitudinal section area was reduced by 17.782% over consecutive iterations to improve crosswind performance. We chose top loading over side loading as it was faster, gave a larger opening and did not require the removal of trusses. The tail section was tapered at  $11.917^\circ$  to prevent tail-strikes and reduce overall drag. We ran multiple CFD analyses to optimize the aerodynamic covers reducing the wake region, vortices and drag, helping the aircraft attain the required take-off velocity. We added vortex generators for the same, ensuring that the wake region does not affect elevator & rudder performance.

### 3.3.3 Vertical Tail (VT)

With the increased Fuselage longitudinal section, high degree of yaw control was required. The team initially used a U Tail to avoid the Fuselage wake region, which we later combatted (**Section 3.3.2**). We finalized chose a conventional tail for its low empty weight. We sized the tail by

calculating the required tail volume coefficient (0.06), analyzing crosswinds at the competition site. NACA 0009, a symmetrical airfoil was selected for its low drag at 0° angle of attack.

### 3.3.4 Horizontal Tail (HT)

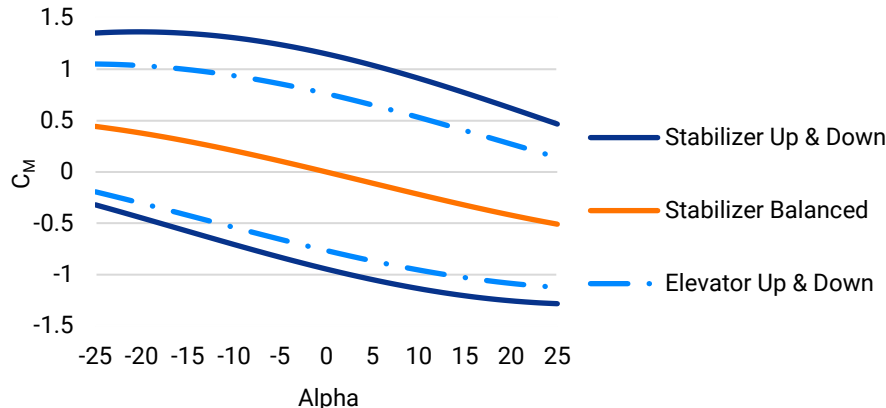


Figure 3(i): C<sub>M</sub> vs Alpha

To achieve a balanced and positively stable empty and loaded CG position, the team calculated and balanced the resulting moments of each force acting on the aircraft.

The tail sizing and inverted asymmetrical airfoil AH 79-100 C were chosen to achieve the required level of pitching moment and negative slope for C<sub>M</sub> versus Angle of Attack.

### 3.3.5 Avionics

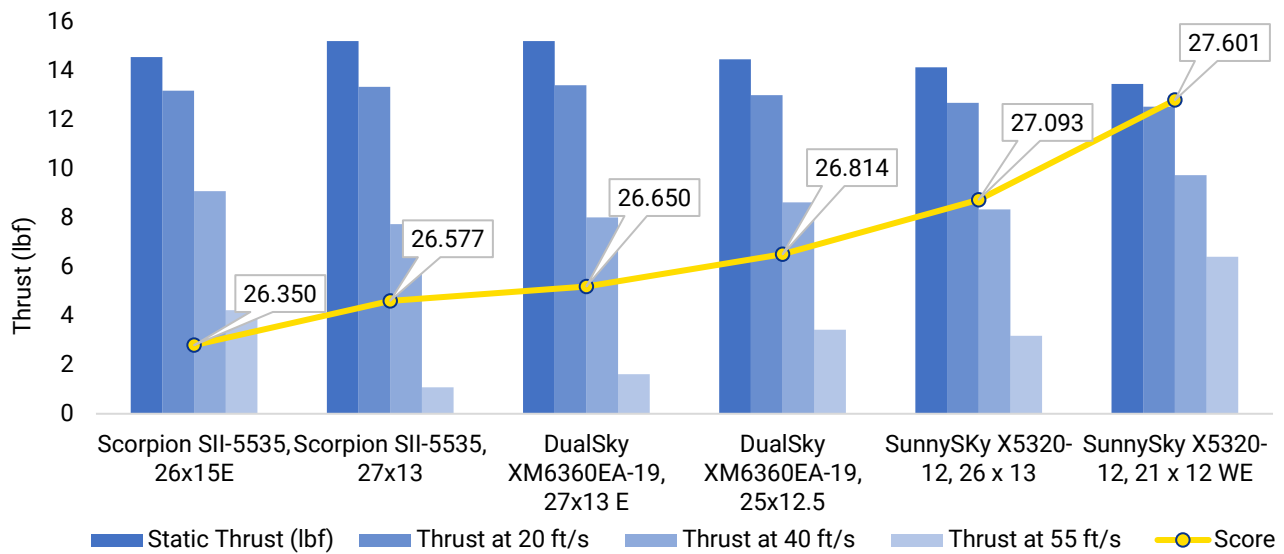
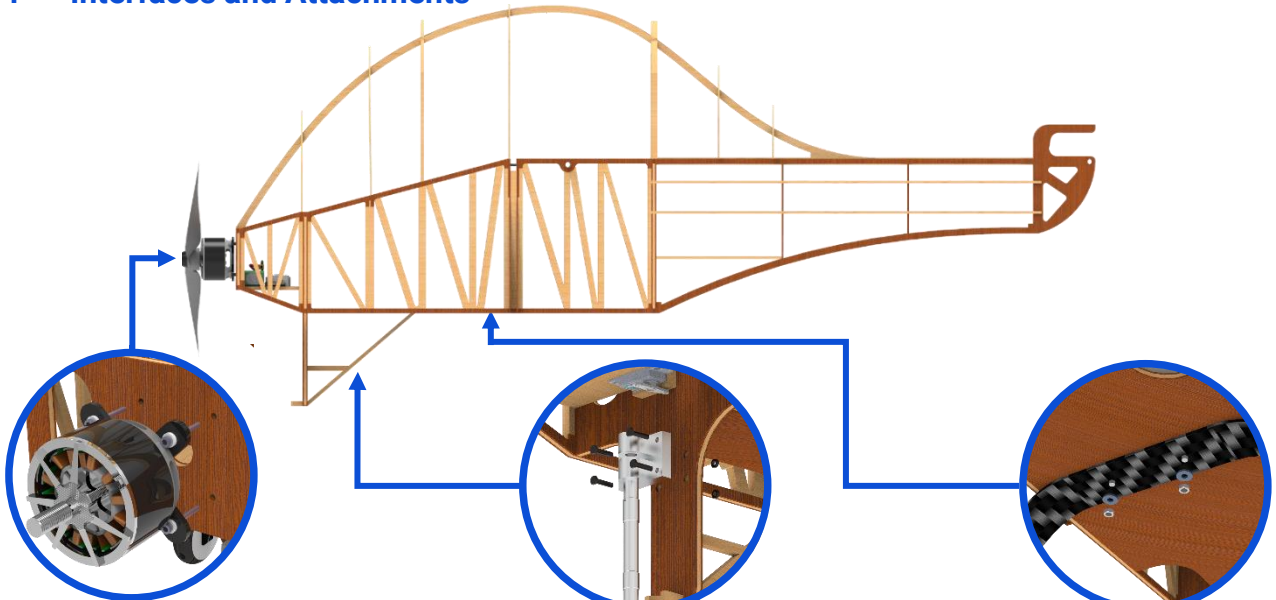


Figure 3(j): Motor-Propeller Combinations

The selection of motor-propeller was based on dynamic performance analysis for the flight conditions of take-off, turning and cruising. The Scorpion's high static thrust of 15.376 lbf. and its benefits to lifting larger all-up weights are nullified by it being double the weight of the SunnySky, requiring higher reinforcements to sustain the higher loads and inferior dynamic performance.

### 3.4 Interfaces and Attachments



**Motor Mounting**

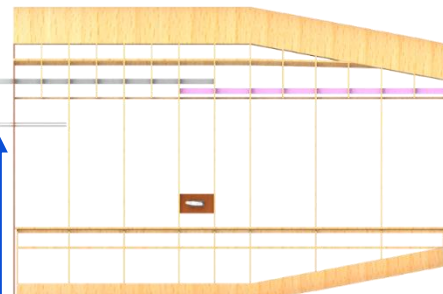
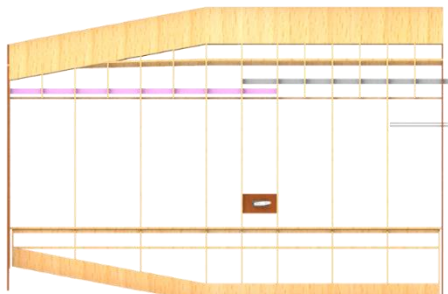
The firewall made from laminate of basswood ply and balsa is used to attach the motor to the fuselage.

**Nose Landing Gear Mounting**

A Delrin bush mounted on a modular plate is used to attach the nose landing gear to a thick laminate rib.

**Main Landing Gear Mounting**

Landing gear bolted to a thick composite baseplate in the lowest deck of the fuselage.



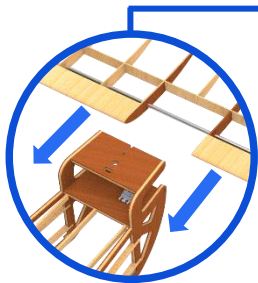
**Primary Spar Locking**

Bolting through co-axial holes in plywood formers of the mid-section on aligning with the primary spar.



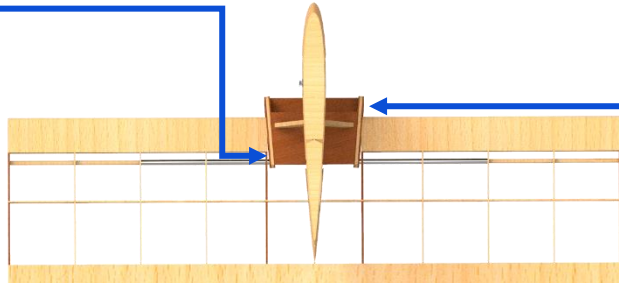
**Rear Spar**

Hollow aluminum rod passed through the wing root section and into longerons.



**Horizontal Stabilizer Mounting**

Mounted using cylindrical main spar entering from the side at the aft end of lower tail plate.



**Vertical Stabilizer Mounting**

Mounted on the top of the elevated tail plate, using bolts.

## 4.0 Loads, Environments and Assumptions

### 4.1 Design Load Derivations

#### 4.1.1 V-n Diagram

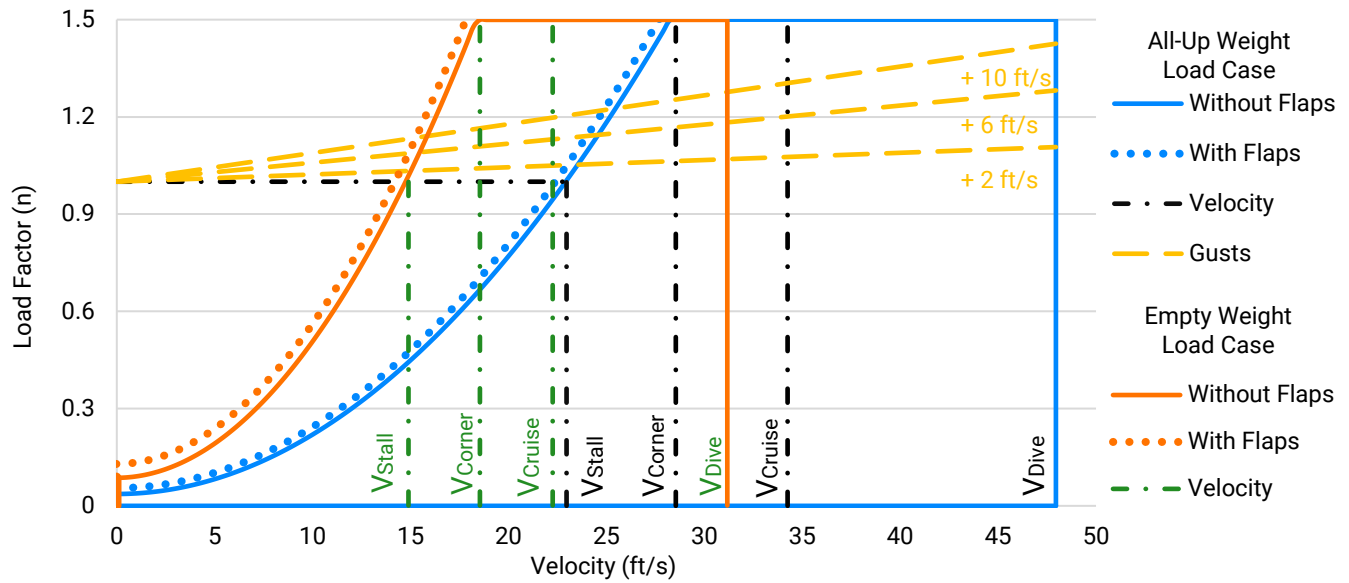


**Figure 4(a): V-n Diagram**

The V-n diagram is generated for empty and all-up weight of the aircraft. The load factor is non-zero when the aircraft is stationary because of propwash. Flaperon deployment extends the flight envelope of the aircraft, as can be seen by the dotted lines. Gust velocities of 2ft/s, 6ft/s and 10ft/s were also considered for the all-up weight load case.

#### 4.1.2 Landing Shocks

Glideslope	Sink Rate	Impact Loading (lbf)
3°	1.1294104	138.3527764
5°	1.8808217	230.4006622
10°	3.7473293	459.0478348

**Table 4(b): Landing Shock Calculations**

The team calculated the impact loading on the airframe during touchdown for glideslopes of 3°, 5° and 10° by calculating change in momentum and normal force. We used telemetry data to derive the former and calculate approach velocity. We recorded the median impact time as 0.2 seconds from multiple flight tests. The fuselage baseplate was designed with a FoS of 1.086 keeping these loads in mind.

## 4.2 Environmental Considerations

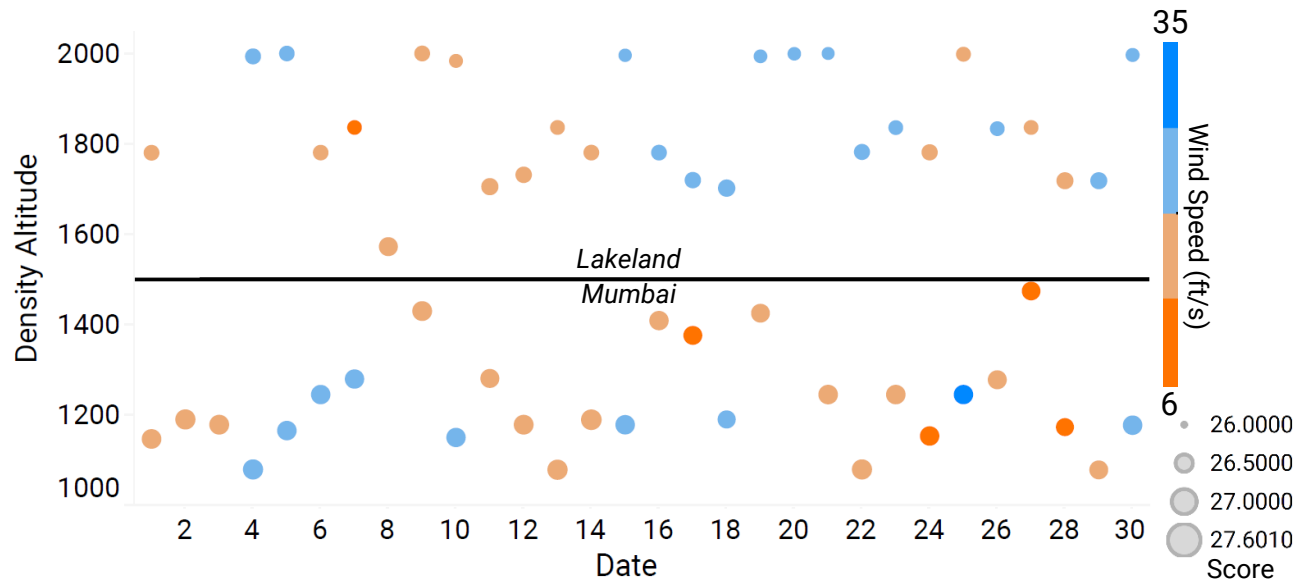


Figure 4(c): Environmental Considerations

We calculated the scores for Mumbai and Lakeland over a period of a month (February for Mumbai, June for Lakeland) which were derived from the density altitudes, taking into account various environmental factors such as temperature, pressure, relative humidity, dew point and altitude during the days of the competition as well as our testing period. We also took into account differing values of rolling resistance at Mumbai and Lakeland. The highest score obtained in Lakeland is 27.183 points with a decrease in score by 1.511% compared to Mumbai.

## 5.0 Analyses

### 5.1 Analytical Tools

#### 5.1.1 Solidworks and XFLR5

The team used Solidworks for CFD and Finite Element Analysis (FEA) over aerodynamic surfaces and load bearing components, respectively. We used topology optimization techniques to achieve the highest overall strength to weight ratio and provide insight into system level structural inadequacies. Solidworks was also used for accurate balancing of masses and CG. We used XFLR5 to interpolate airfoils and to export their polars. It was also used for obtaining and analyzing static and dynamic stability eigenvalues.



### 5.1.2 Tableau & Microsoft Excel

Used to generate detailed and efficient graphs and plots with varying scores, wingspan, cargo configurations, aspect ratios and payload showing how we optimized those parameters.

### 5.1.3 MATLAB

MATLAB Module Tornado VLM was used for analyses of wing planforms in order to obtain  $C_L$  and  $C_D$  values, while the Global Optimization Toolbox by MathWorks was used to optimize the above system variables using the advanced technique of genetic optimization to find the global maxima with score being the fitness value.

## 5.2 Developed Models

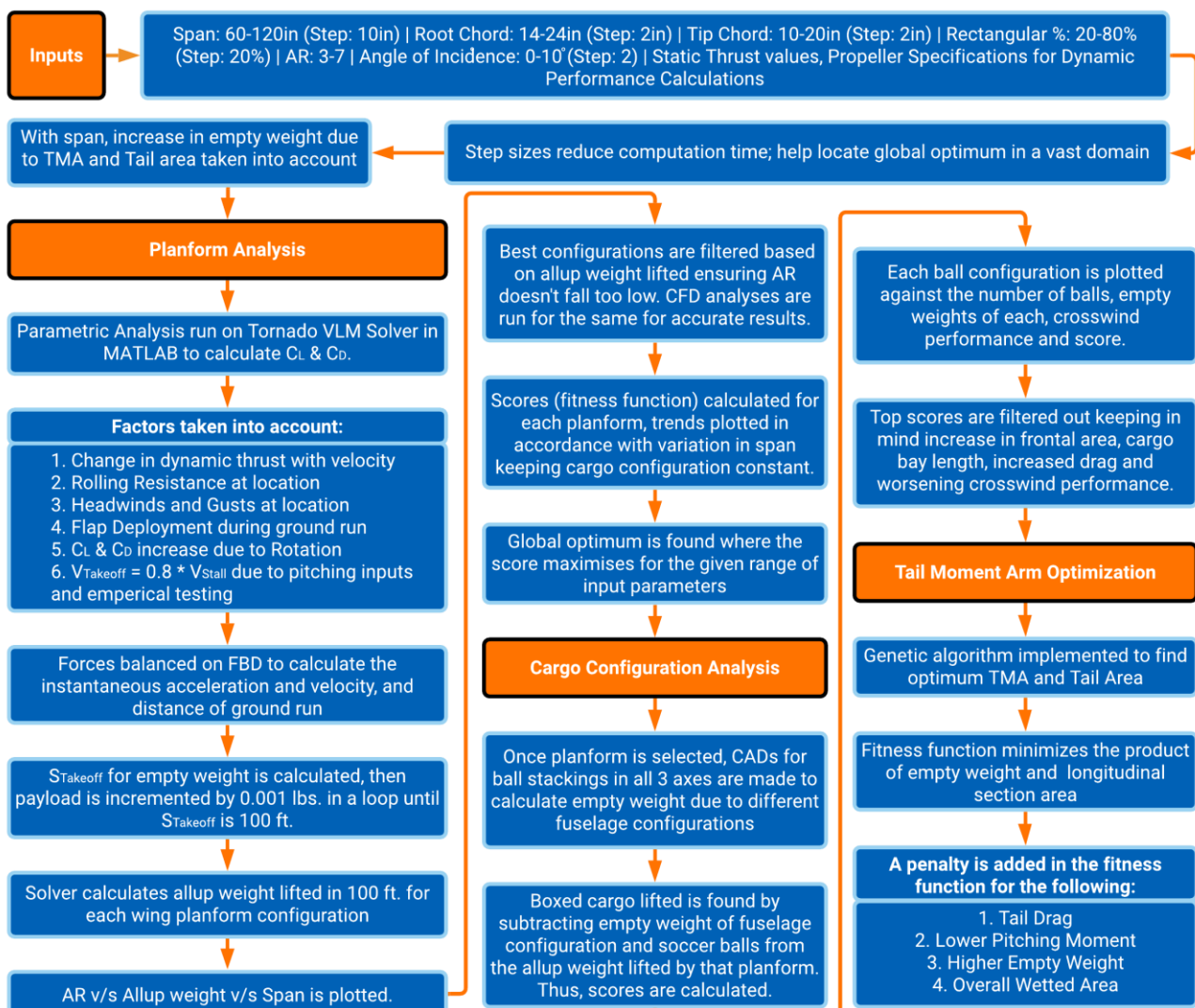


Chart 5(a): Developed Models

## 5.3 Performance Analyses

### 5.3.1 Dynamic Thrust

We analyzed the dynamic thrust characteristics of various motor propeller combinations (**Section 3.3.5**), as described in **Section 6.0**. Figure 5(b) compares three best combinations showing payload lifted against take-off distance. We prioritized dynamic thrust over high static thrust allowing for flight in high degrees of headwinds.

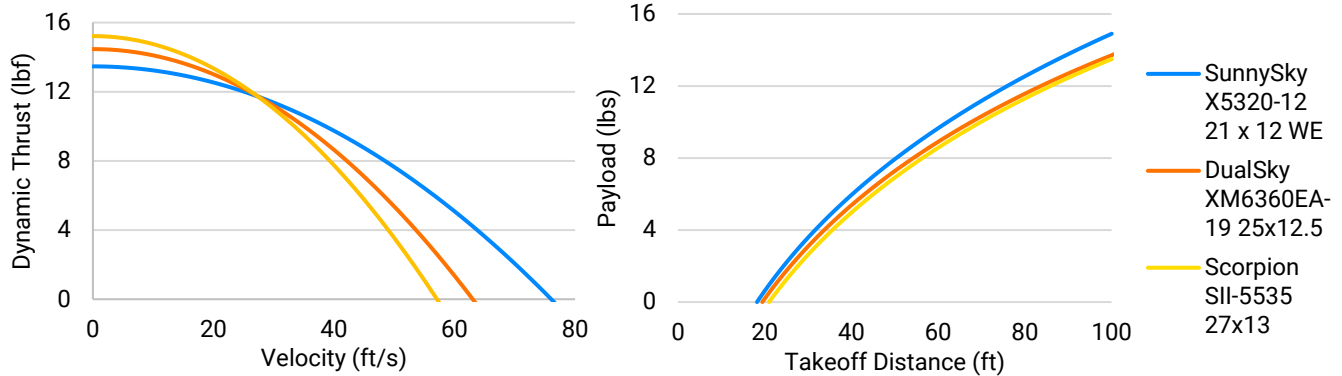


Figure 5(b): Dynamic Thrust Performance

### 5.3.2 Take-off and Climb Out Performance

We incorporated equations governing take-off in our calculator, running simulations for each iteration of our aircraft. Below are the trajectories of the best flight of our 4 prototypes derived from telemetry obtained after empirical testing along with a summary of our development cycle.

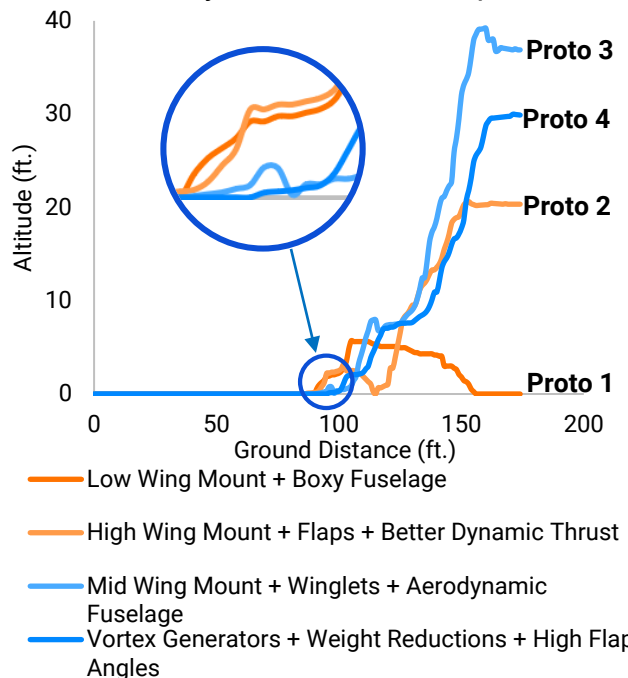


Figure 5(c): Take-off and Climb-out Telemetry

Proto	Pros	Cons	To Improve
1	Lifted 22.5lbs assisted by high ground effect.	Unable to retain in-flight velocity - low thrust. Unstable.	Make fuselage aerodynamic, increase dynamic thrust and stability
2	Lifted 23.2 lbs. Retained velocity in air. Flaps increased lift.	Changed to heavier, more powerful motor caused nose down. Difficulty in rolling.	Increase TMA, tail area to balance pitching moments. Increase propwash effect.
3	Lifted 24lbs as high lift due to propwash. Stable flight.	High empty weight, FoS and structural redundancy	Perform weight reductions, reduce wing and fuselage wake
4	Lifted target 24.5 lbs. Stable flight.	Unable to lift any more, crash at 25lbs.	Final config set to 24.5lbs as the top scoring test flight.

Table 5(d): Post Flight-Test Optimizations

### 5.3.3 Flight and Maneuver Performance

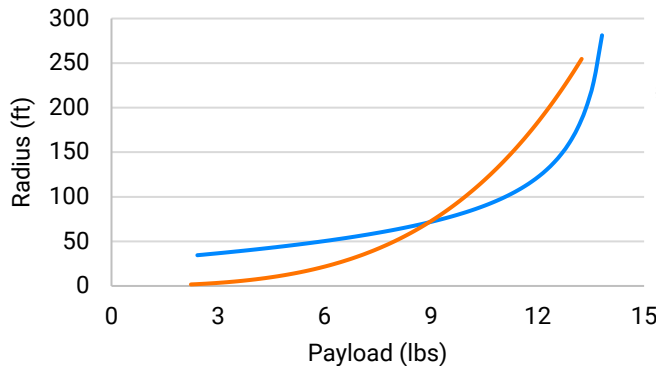


Figure 5(e): Minimum Turning Radius

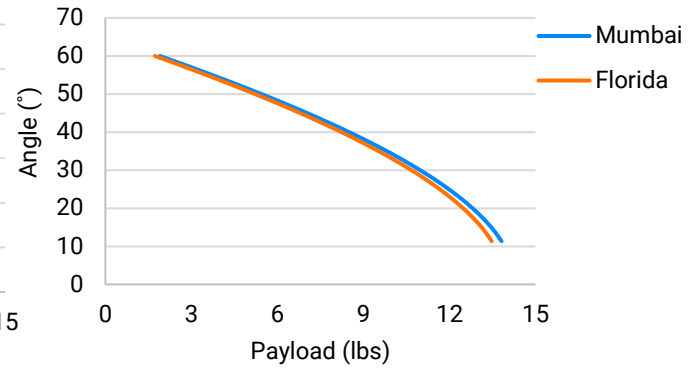


Figure 5(f): Maximum Banking Angle

The team calculated the maximum banking angles and turning radii for various load factors and velocities; by resolving the forces acting on the free-body diagram of the aircraft. The graphs represent variation in these factors depending on air densities at their respective locations.

### 5.3.4 Static and Dynamic Stability

The negative slope of the aircraft (Figure 3(i)) indicates that the aircraft is statically stable. The neutral point is 21.35" from the aircraft datum and the static margin is 7.37% of Mean Aerodynamic Chord.

Oscillating Aircraft Dynamic Response		
Aircraft Motion	Damping Factor	Oscillation Time (seconds)
Short Period (Longitudinal)	0.612	1.161
Phugoid (Longitudinal)	0.029	5.747126437
Dutch Roll (Lateral)	0.604	1.153
Non-oscillating Aircraft Dynamic Response		
Roll Dampening (Lateral)	Tau: 0.043	Dampening Time: 0.624 seconds
Spiral Instability (Lateral)	Pilot Response Time: 2 seconds	Pitch Rate at Response Time: 82.378 °/s

Table 5(g): Stability Response

Dynamic stability was ensured in adverse conditions by maintaining a FoS of 1.2 on all control surfaces allowing for the aircraft to be controllable in all axes.

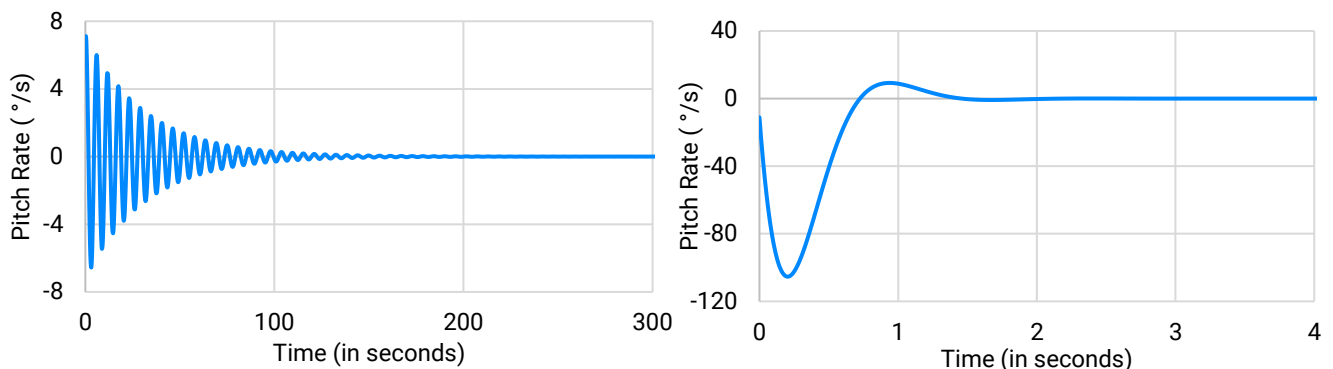


Figure 5(h): Short Period and Phugoid Modes

Roll Dampening	-23.24555	Dutch Roll	-3.28982+4.34199i	Spiral Instability	0.72959
----------------	-----------	------------	-------------------	--------------------	---------

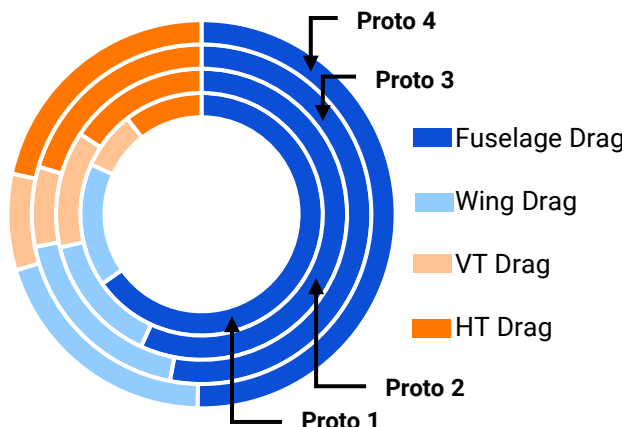
Table 5(i): Lateral Stability Eigenvalues

### 5.3.5 Payload Prediction Analysis

The payload lifted at different density-altitudes (DA) was calculated by the following formulae:

All-up weight lifted =  $L$ ;  $L = \left(\frac{1}{2}\right) \cdot C_L \cdot \rho \cdot S \cdot v^2$ ;  $P = L - 10.5$ ; where  $P$  is the payload lifted. We made a DA calculator which, at standard conditions, output the ideal pressure and temperature, and consequently the density at different altitudes. The DA at the test site and all-up weight was calculated by empirical testing. The value of the base all-up weight lifted at a DA of 0ft was then reverse engineered, the data then being extrapolated in a range of 0 to 10000 ft. to find the all-up and the payload that could be carried at that DA. The equation of the line plotted from this data is:  $y = -0.00067241x + 15.2117285$

### 5.3.6 Drag Polar Analysis



The team calculated the percentage drag contributions of major components of the aircraft over four prototype designs, as shown here. A significant decrease in the drag of the fuselage was obtained over the course of these iterations.

## 5.4 Structural Analyses

Figure 5(j): Drag Polar Analysis

### 5.4.1 Critical Margins

Material	Component/Condition	Max Stress Induced (PSI)	Max Allowed Stress (PSI)	FoS
Balsa	Stringers	1753.28	1914.5	1.092
Basswood	Baseplate during cruise	2091.12	2264.1	1.083
	Baseplate while turning	2104.33	2264.1	1.076
Aluminium	Wing Dowel during cruise	18699.2	26933.5	1.440
	Wing Dowel while turning	21940.27	26933.5	1.228
XPS Foam	Wing Insert during cruise	399.76	843.52	2.110
Mild Steel	Wing Locking during cruise	34192.62	53664	1.569
	Wing Locking while turning	35371.2	53664	1.517

Table 5(k): Material Selections

## 5.4.2 Applied Loads and Material Selection

### 1) Tail Force Analysis

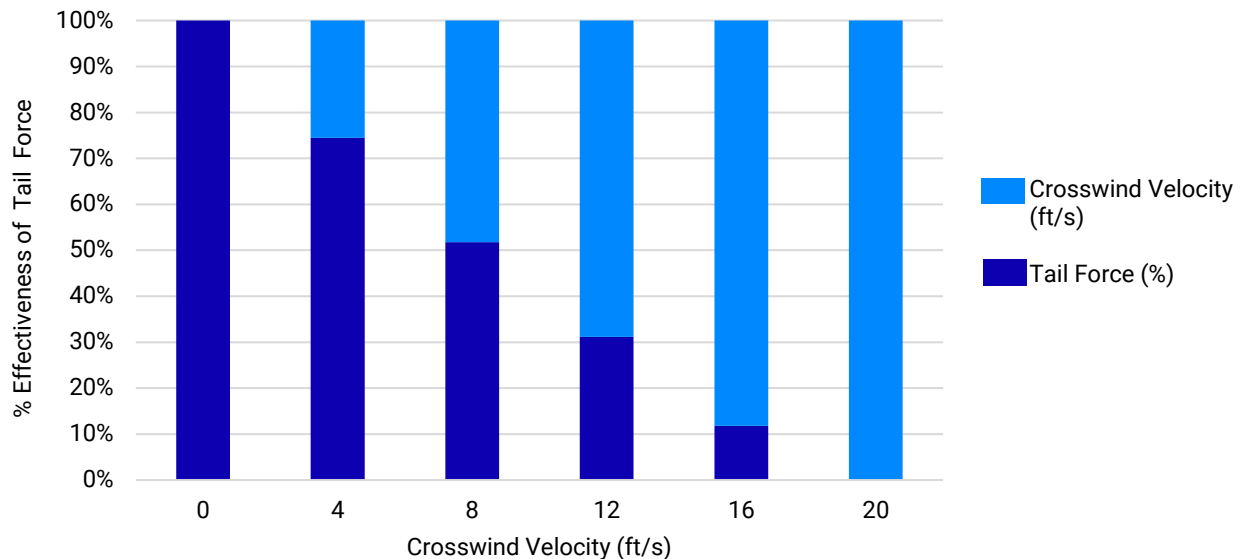


**Figure 5(l): Crosswinds Analysis**

The team analyzed rudder performance under crosswind conditions by developing a mathematical model where rudder forces were measured by varying crosswind intensity during flight. The rudder becomes ineffective at 18.6 ft/s. Since Lakeland has an average wind speed of 9.2 ft/s, the rudder will perform at 40-50% effectiveness.

### 2) Material Selection

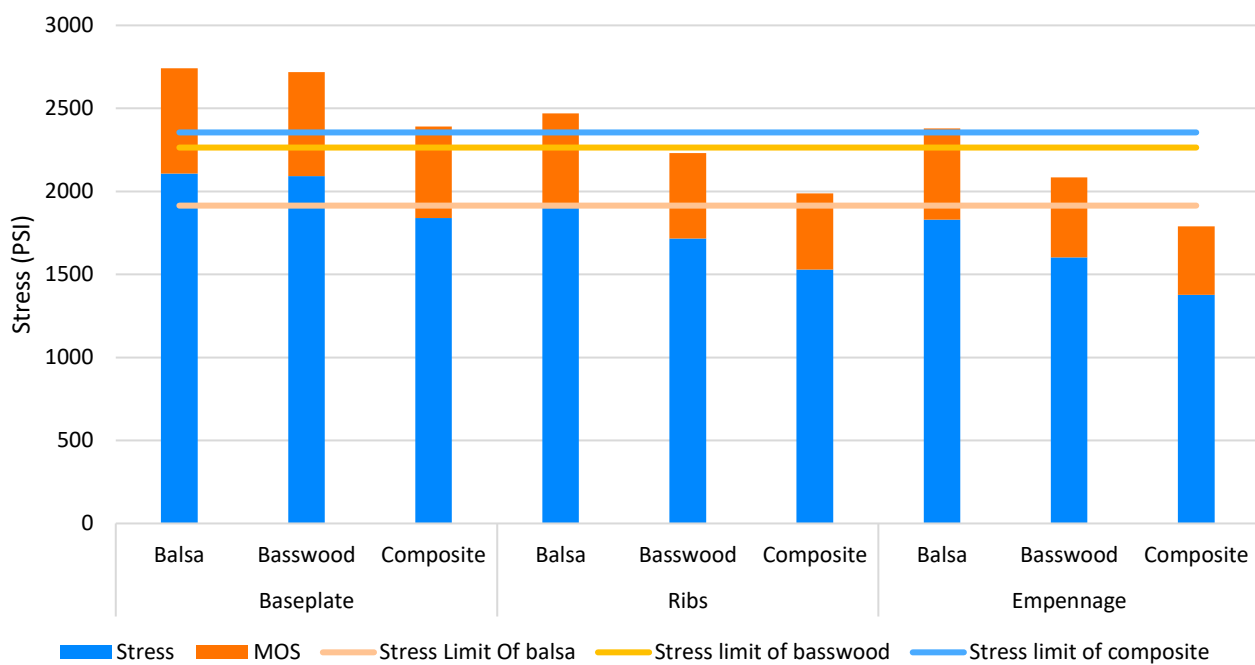


**Figure 5(m): Composite Stress Analysis**

We constructed the airframe primarily with wood, with the main wing spar made of a hollow rectangular cross-section aluminum beam in the center and XPS foam in the outer half due to aluminum's anisotropic strength, high endurance, greater resistance to shear and bending forces, and the foam's immense Strength to Weight (S/W) Ratio. Balsa was used in the wing and tail sub-assemblies for its low density and high S/W ratio. We used basswood at regions of concentrated loads, especially junctions between components. Laminates of balsa and basswood were used for the ribs, baseplate and longerons as they offer significantly higher strength than balsa, strengthening critical areas while being lighter than conventional hardwood.

### 3) Mass Properties & Balance

#### A. Centre of Gravity

Based on our calculations and pilot inputs, the aircraft was designed with the CG 3.11" in front of the Neutral Point ensuring static stability. The main landing gear was placed near the CG to aid in equal weight distribution and prevent excessive loading on the nose landing gear.

#### B. Weight Distribution

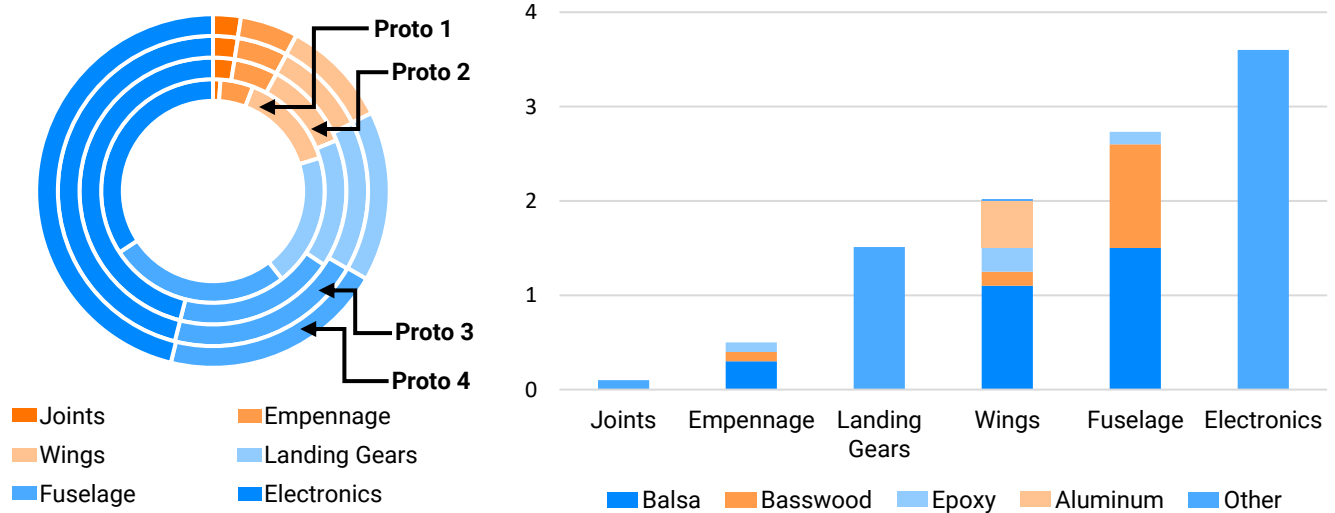


Figure 5(n): Weight Distribution

To minimise empty weight, each component, as well as the 2-part epoxy was weighed before implementation. Weight reductions were done in components with lesser critical loading while reinforcing regions requiring a high FoS. Empty weight was reduced with each iteration.



## 6.0 Sub-Assembly Tests and Integration

### 6.1 Propulsion System Testing

The team shortlisted motors-propeller combinations after comparing thrust values from eCalc, limiting them to 1000W. The motor mount was attached to the free end of a load cell mounted vertically on a pedestal. Data was calibrated and logged using Arduino UNO. We attempted to measure dynamic thrust using a rudimentary wind tunnel setup comprising counter rotating fans at the outlet of a diffuser with a 2" honeycomb straw structure and stainless-steel mesh screen in the contraction cone (plywood) to generate laminar airflow. A smoke system was used to view flow trajectories through a plexiglass screen. We compared values with eCalc and reverse engineered past flights finding the median error of the setup to be 4.52%.

### 6.2 Battery and Servo Testing

Battery endurance was tested by operating the motor statically at full throttle for the time taken to complete 2 flight rounds. We verified these results during flight tests for the same scenario.

Control Surface	Servomotor	Rated Torque (oz-in)	Control Surface Deflection	Torque Required (oz-in)
Flaperon	Turnigy MX355WP	166.648	30°	60.775
Elevator	Turnigy WP23	319.409	30°	116.38
Rudder	Turnigy TGY 813	124.986	30°	27.83
NLG	Turnigy WP23	319.409	30°	250.17

Table 6(a): Servo Torque Requirements

### 6.3 Materials and Loads Testing

We performed Universal Testing Machine operations on longerons, wing spar cross-sections, alternate materials and structures to identify ultimate and shear stress values. Structural loading at critical junctions was calculated to design structural members.

### 6.4 Flight Testing

We tested various design configurations equipped with RPM and GPS sensors, accelerometer, Pitot tube and altimeter to gather telemetry data. We conducted flights with an incremental weight build-up strategy, with the maximum lifting capacity judged from pilot feedback.



## 7.0 Manufacturing

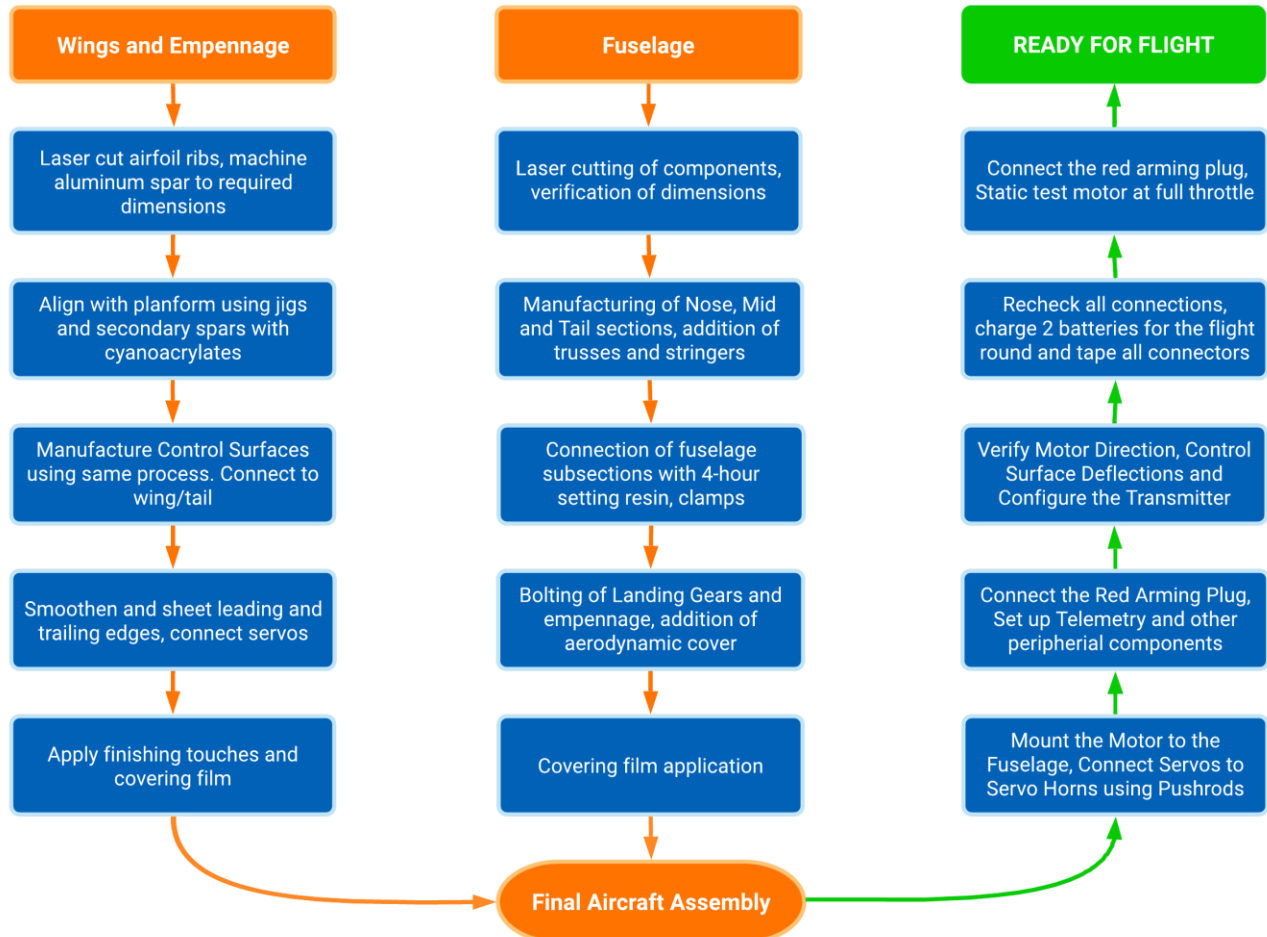


Chart 7(a): Manufacturing Process

## 8.0 Conclusion

The designed aircraft can carry 4 spherical and 10.5 lbs. of boxed cargo with the unique combinations of materials used ensuring structural soundness and extensive empirical testing backing our calculations. With circumstances like these, we consider ourselves fortunate to be participating this year, and expect to be competitive at SAE Aero Design Validation, 2021.

### References:

1. Anderson, John D., "Introduction to Flight: Its Engineering and History."
2. Caughey, David A., "Introduction to Aircraft Stability and Control Course Notes"
3. Nicolai, Leland M., and Grant Carichner., "Aircraft Design"
4. Sadraey, Mohammad H., "Aircraft Design: A Systems Engineering Approach"
5. Team 024, DJS Skylark - Regular Class Design Report, SAE Aero Design East, 2020.



## Appendix A – Backup Calculations

### Takeoff Equation: (SECTION 5.3.2)

$$S_{To} = \frac{1}{2B} \ln \left| \frac{A}{A - Bv^2} \right| ; \text{ Where, } A = \left( \frac{T_s}{W} - \mu \right) ; \quad B = \frac{g}{\omega} \left[ \frac{1}{2} \rho S (C_D - \mu C_L) + \alpha \right] ; \quad \alpha = 0.11126$$

### Thrust Equations: (SECTION 3.3.5)

$$T_d = T_s - \alpha v^2 ; \quad \text{When } T_d = 0, \quad T_s = \alpha v_e^2 , \quad \alpha = \frac{T_s}{\left( \frac{\text{RPM}_{\text{motor}}}{60} \times \text{pitch}_{\text{propeller}} \times 0.0254 \right)^2}$$

### Turning Radius Calculations: (SECTION 5.3.3)

$$\text{Radius} = \frac{mv^2}{L \sin \phi} ; \quad \text{Banking Angle } (\phi) = \cos^{-1} \left( \frac{W}{L} \right)$$

### Servo Torque Calculations: (SECTION 6.2)

$$\frac{\text{Servo Torque Required}}{} = (8.5 \times 10^{-6}) \frac{C^2 \times v_d^2 \times \text{control surface span} \times \sin^2(S_1)}{\cos(S_1) \times \tan(S_2)} \times \frac{\text{control horn height}}{\text{servo arm length}}$$

### Aircraft Corner Speed (V\*): (SECTION 4.4.1)

$$V^* = \sqrt{\frac{2n_{\max}mg}{\rho S C_{L_{\max}}}}$$

### Gust Induced Load factor: (SECTION 4.4.1)

$$n = 1 + \frac{k_g v_g E V_E \alpha \rho S}{2mg}$$

### Bending Stress and Landing Shocks: (SECTION 5.4.2 AND 4.1.2)

Bending Stress/y = Bending Moment/I ; Where, y=⊥ distance from NA, I=Moment of inertia

Impact = Normal Reaction + Impulse ; Impulse= Momentum/Impact time

### Drag Polar: (SECTION 5.3.6)

$$C_D = C_{D0} + C_{Di} ; \quad C_{Di} = C_L^2 / (\pi \times AR \times e) ; \quad C_{D0} = C_{D0(\text{fuse})} + C_{D0(\text{wing})} + C_{D0(\text{Hstab})} + C_{D0(\text{Vstab})}$$

$$C_{D\min(\text{surface})} = C_f(\text{surface}) \times \text{Form Factor}_{(\text{surface})} \times \frac{\text{wetted area}}{\text{reference area}} ; \quad \text{Where, } e = \text{Efficiency Factor}$$

### Climb Out: (SECTION 5.3.2)

$$\theta = \cos^{-1} \left( \frac{0.5 \rho C_L S v^2}{mg} \right) ; \quad v_y = v_x \tan \theta ; \quad v = (v_x^2 + v_y^2)^{0.5}$$

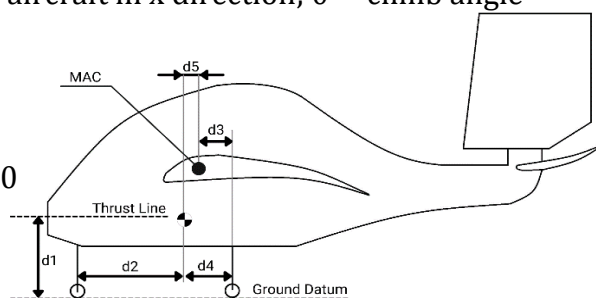
$v_y$  = velocity of aircraft in y direction;  $v_x$  = velocity of aircraft in x direction;  $\theta$  = climb angle

### Moment Equations: (SECTION 5.3.4)

$$\text{On-ground} \quad T_s d_1 - W d_2 = 0$$

$$\text{Take-off} \quad T_d d_1 - L d_3 + W d_4 - L_{T_1} (TMA - d_4) = 0$$

$$\text{In flight} \quad L_w \times d_5 = L_{T_2} \times TMA$$





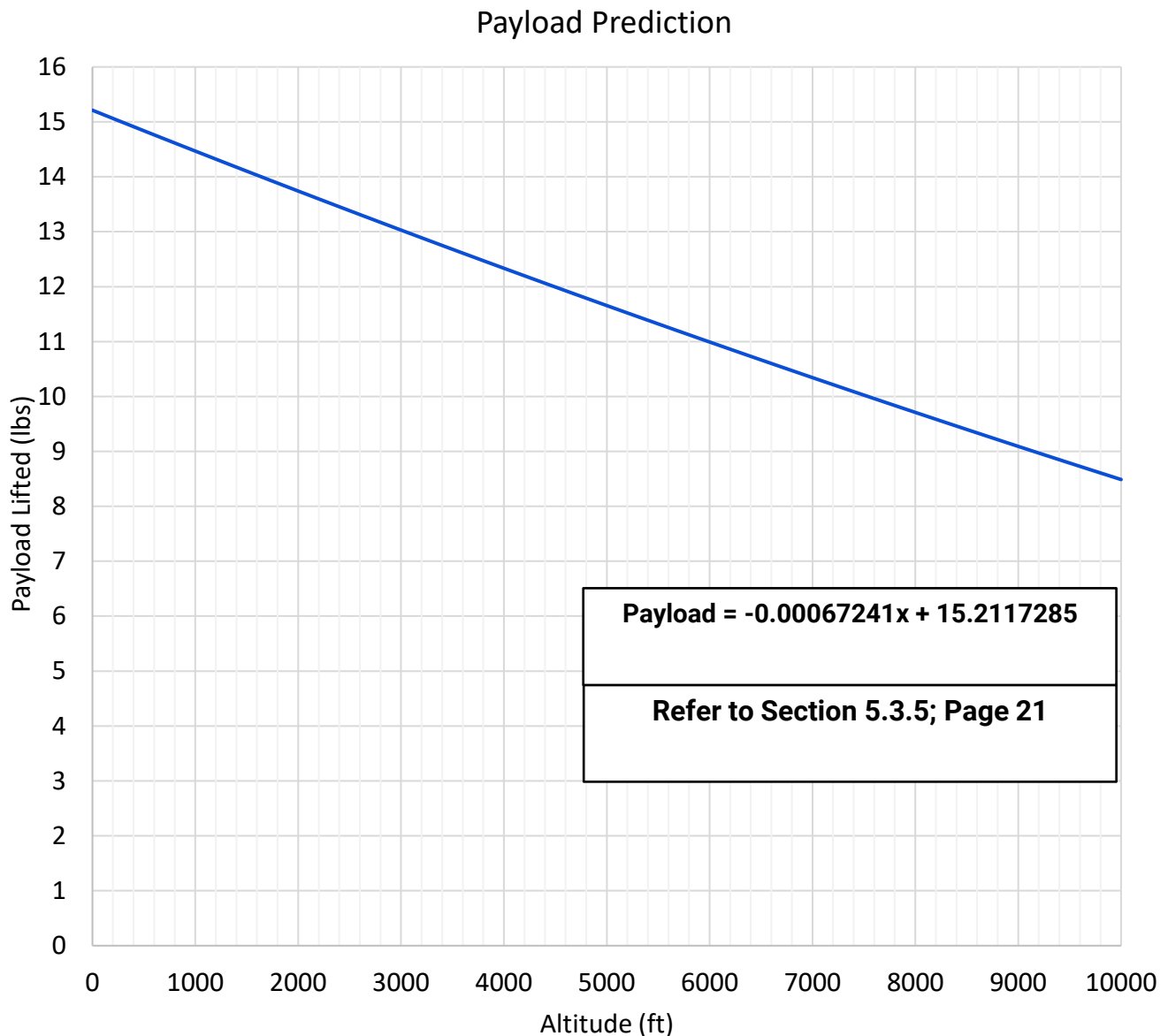
## Appendix B – Technical Data Sheet

### Payload Prediction Curve (Regular Class)

**Team Name:** DJS Skylark – REGULAR CLASS

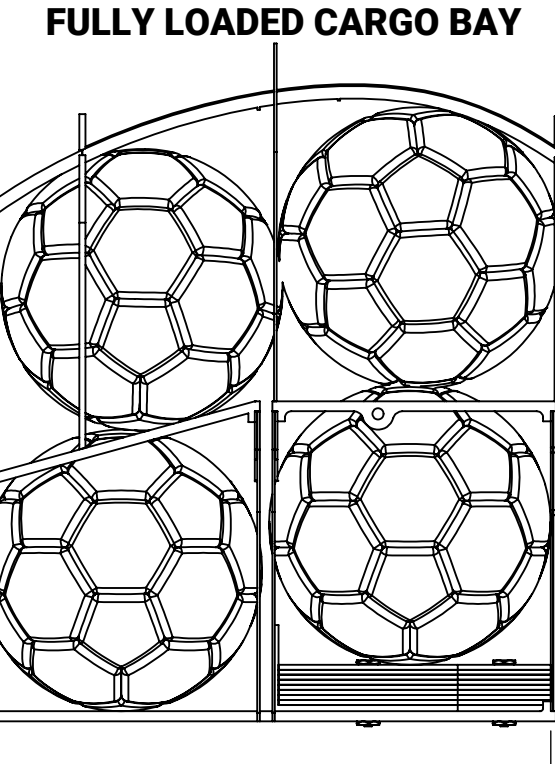
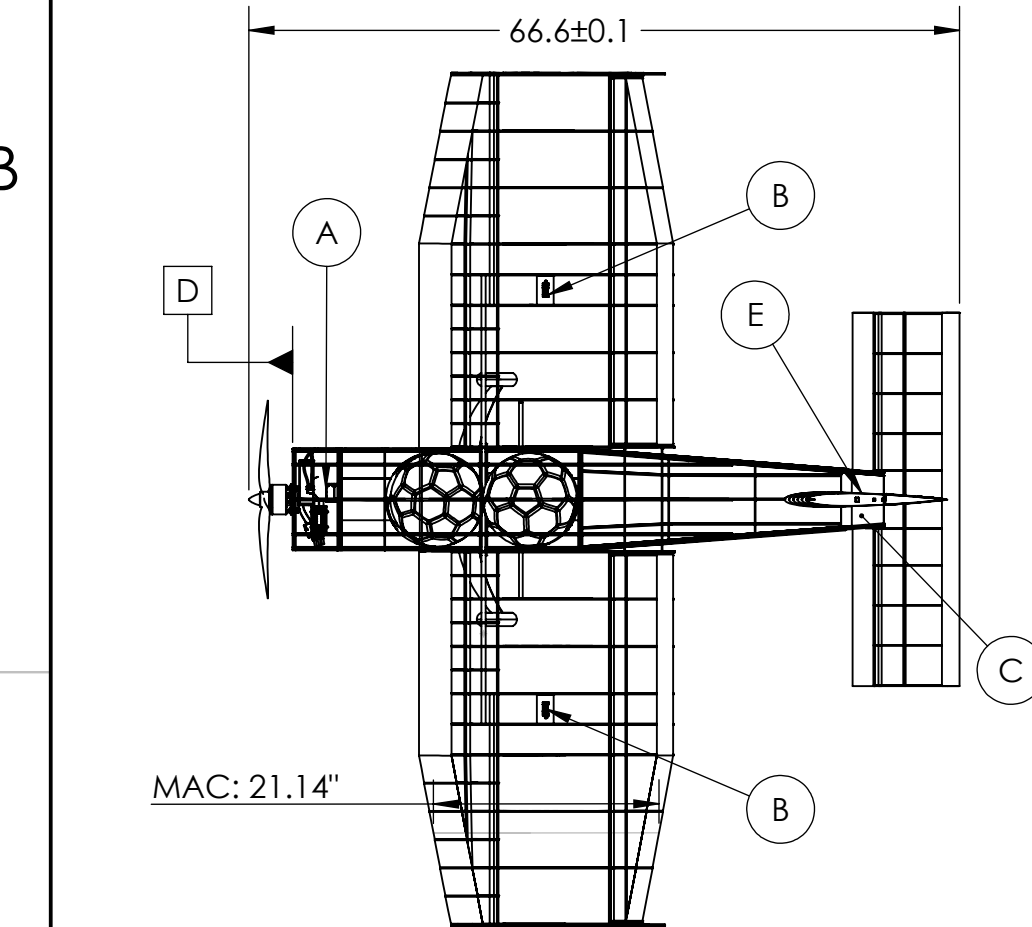
**Team Number:** 019

**School Name:** Dwarkadas J. Sanghvi College of Engineering

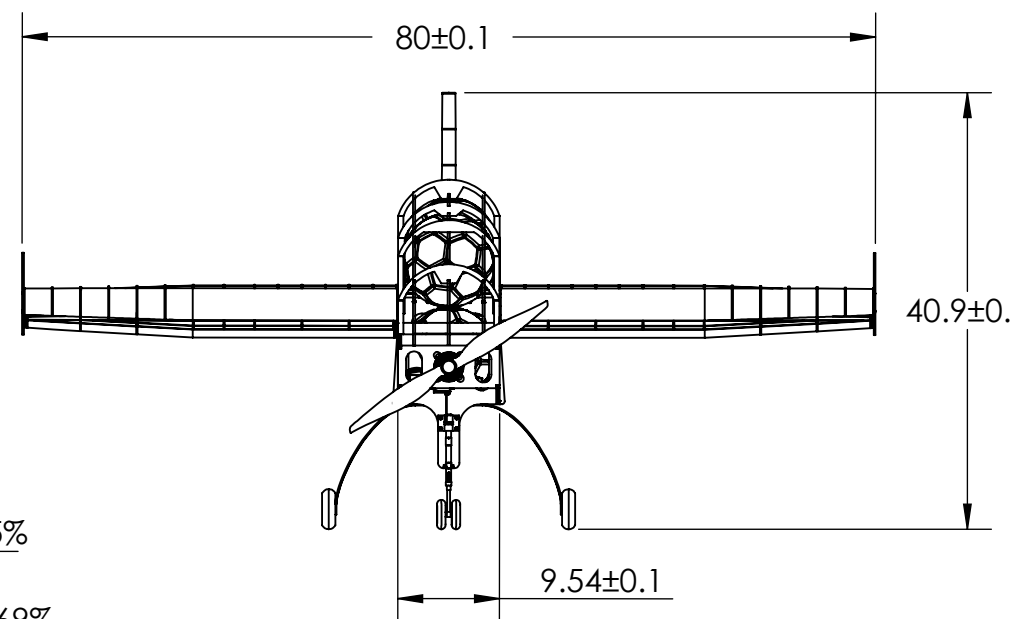
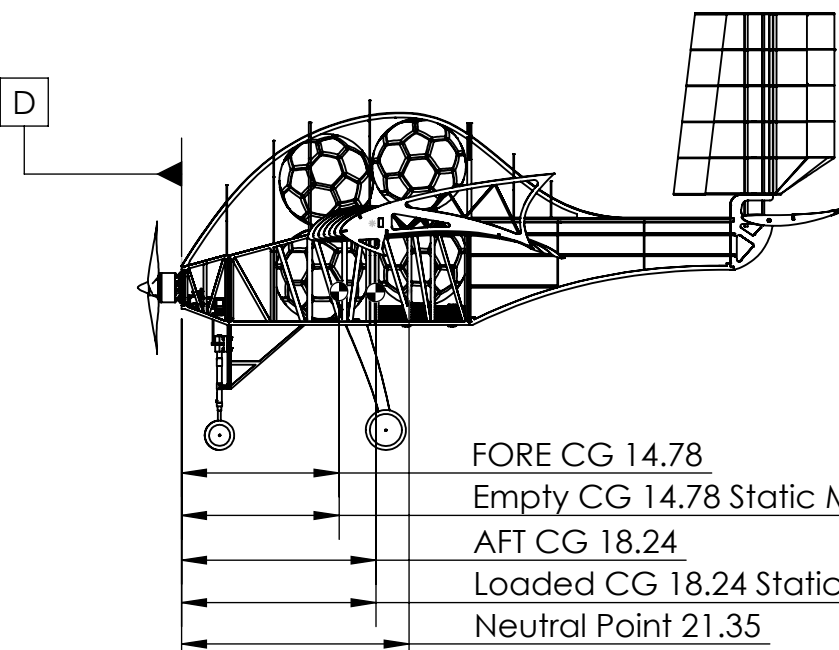


### AIRCRAFT SUMMARY DATA

WINGSPAN	MAC	TMA	EMPTY WEIGHT	BATTERY	MOTOR MODEL	MOTOR KV	PROPELLER	SERVO (Nose Landing Gear) (A)	SERVO (Flaperon) (B)	SERVO (Elevator) (C)	SERVO (Rudder) (E)
80 ± 0.1"	21.14"	36 ± 0.1"	10.5 lbs	Tattu LiPo 3300mAh 6S	SunnySky X5320 12-14 poles	250KV	APC 21x12WE	Turnigy WP23 (319.41oz-in)	Turnigy MX-355 WP (166.64 oz-in)	Turnigy WP23 (319.41oz-in)	Turnigy TGY 813 (124.99oz-in)



SCALE 1:6



### WEIGHT & BALANCE

SR. NO.	COMPONENTS	WEIGHT (lbs)	ARM (in.)	MOMENT (lbs-in)
1)	MOTOR	1.186	1.928	2.287
2)	BATTERY	1.034	1.555	1.608
3)	PAYOUT	10.5	21.88	229.74
4)	ELECTRONICS	0.655	2.078	1.361
5)	SPH. CARGO	3.5	18.119	63.416

### BASIC DIMENSIONS

LENGTH	66.6 ± 0.1"
WIDTH	80 ± 0.1"
HEIGHT	40.9 ± 0.1"

Team NO: 019  
Team Name: DJS Skylark - REGULAR CLASS  
  
School Name: Dwarkadas J. Sanghvi College of Engineering  
  
SAE Aero Design Knowledge 2021  
  
Size: B Scale: 1:18 Unit: inches